DOT/TSC-RA-3-8-3

Project Report
ATC-26 III

Technical Assessment of Satellites for CONUS Air Traffic Control Volume III: Satellite-to-Aircraft Techniques

H. B. Lee
B. B. Goode

17 February 1974

Lincoln Laboratory
MASSACHUSETTS INSTITUTE OF TECHNOLOGY
LEXINGTON, MASSACHUSETTS

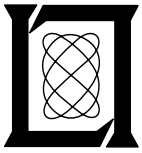

Prepared for the Federal Aviation Administration,
Washington, D.C. 20591

This document is available to the public through
the National Technical Information Service,
Springfield, VA 22161

TECHNICAL REPORT STANDARD TITLE PAGE

1. Report No.	2. Government Accession No.	3. Recipient's Catalog No.
DOT/TSC-RA-3-8-3		

4. Title and Subtitle	5. Report Date
Technical Assessment of Satellites for CONUS Air Traffic Control Vol. III: Satellite-to-Aircraft Techniques	19 February 1974
	6. Performing Organization Code
7. Author(s)	8. Performing Organization Report No.
H. B. Lee and B. B. Goode	ATC-26 Volume III
9. Performing Organization Name and Address	10. Work Unit No.
Massachusetts Institute of Technology Lincoln Laboratory P. O. Box 73 Lexington, Massachusetts 02173	11. Contract or Grant No. DOT/TSC-RA-3-8
	13. Type of Report and Period Covered
12. Sponsoring Agency Name and Address	Project Report
Transportation Systems Center Department of Transportation 55 Broadway Cambridge, Massachusetts 02142	14. Sponsoring Agency Code

15. Supplementary Notes

The work reported in this document was performed at Lincoln Laboratory, a center for research operated by Massachusetts Institute of Technology.

16. Abstract

A number of satellite system techniques have been suggested as candidates to provide ATC surveillance, communication, and/or navigation service over CONUS. All techniques determine the aircraft positions by multilateration based on the arrival times of signals transmitted between the aircraft and the satellites. The techniques can be categorized as follows: (1) Coordinated Aircraft-to-Satellite Techniques (CAST), (2) Random Access Aircraft-to-Satellite Techniques (RAST), (3) Satellite-to-Aircraft Techniques (SAT).

This three-volume report is a technical assessment of all three techniques. The present volume examines satellite-to-aircraft techniques (SAT). The remaining two volumes treat CAST and RAST.

The assessment has shown that workable systems could be configured using any one of the three techniques without reliance on high risk technology. No one technique has emerged as superior. Rather several viable alternatives have been identified. All techniques appear to require more costly avionics than today's ground-based system.

17. Key Words	18. Distribution Statement
Air Traffic Control surveillance navigation satellite systems AATMS	Document is available to the public through the National Technical Information Service, Springfield, Virginia 22151.

19. Security Classif. (of this report)	20. Security Classif. (of this page)	21. No. of Pages	22. Price
Unclassified	Unclassified	116	4.25 HC 1.45 MF

Form DOT F 1700.7 (8-69)

CONTENTS

CONTENTS (CONT.)

LIST OF ILLUSTRATIONS

LIST OF TABLES

SECTION I

SUMMARY AND PRINCIPAL CONCLUSIONS

1.1 INTRODUCTION

Over the last half decade a number of satellite system techniques have been advanced as candidates to provide Air Traffic Control (ATC) surveillance, communication and/or navigation service over the CONtinental United States (CONUS) [1-9]. Each technique has its advantages and disadvantages. All employ position location service by multilateration using a constellation of satellites. These techniques can be grouped into three basic categories according to certain key technical features. The three categories are:

Coordinated Aircraft-to-Satellite Techniques (CAST)

> Systems employing these techniques interrogate aircraft sequentially. The response from an aircraft is the transmission of a timing pulse. This pulse is received by the satellites and then relayed to a ground processing facility. The ground processing facility determines the signal time of arrival (TOA) at each of the satellites and estimates the aircraft position by multilateration. The position information is then incorporated into the ATC surveillance data base. The interrogation algorithm is designed to eliminate overlapping signal pulses at the satellites and hence, mutual interference.

Random Access Aircraft-to-Satellite Techniques (RAST)

> Systems employing these techniques have each aircraft transmit a timing pulse which is received by four or more satellites and relayed to a ground processing facility. This facility determines TOA at each of the satellites and estimates the aircraft position by hyperbolic multilateration. The position information is then incorporated into the ATC surveillance data base. Since aircraft transmit in an uncoordinated manner, system performance, i.e., accuracy and update rate, is ultimately limited by mutual interference caused by signal overlap at satellite receivers.

Satellite-to-Aircraft Techniques (SAT)

> Systems employing these techniques operate by having four or more satellites periodically transmit timing pulses to aircraft. A navigation processor (computer) aboard each aircraft determines the aircraft position from the signal TOA. The information also can be data linked to the ground for inclusion in a ground maintained ATC surveillance data base.

This volume is concerned with an assessment of the critical technical aspects of Satellite-to-Aircraft Techniques (SAT). The other two techniques are treated in Volumes I and II [10,11].

These three volumes concentrate only on the crucial technical issues. They do not attempt to assess the broad spectrum of operational or economic implications of employing these techniques in the National Airspace System. Issues such as the cost-effectiveness of satellites as an element in the CONUS ATC system are beyond the scope of these investigations. Detailed questions concerning the manner by which any of these satellite techniques might evolve from present day aircraft surveillance/navigation systems are also outside the scope of this report. Detailed operational requirements that would be imposed upon a satellite system for CONUS ATC have not been given consideration in depth.

The results of the technical assessment of all three satellite techniques have verified that satellite-based techniques for CONUS ATC could be developed without reliance on high risk technology. No one particular technique has emerged as superior; rather, several feasible alternatives have been identified.

One of the primary attractive attributes of satellites is their inherent ability to provide broad coverage of low altitude airspace. Unpressurized general aviation aircraft are predominant users of low altitude airspace.

The anticipated rapid growth in general aviation over the next several decades can be expected to increase the utilization of this airspace. Hence, a central issue is the complexity of general aviation avionics required for satellite operation. It has been concluded that all three of the techniques considered require more complex avionics (for a given user class) than is currently employed for comparable service with a ground-based system.

1.2 HOW SAT WORKS

The basic satellite-to-aircraft technique (SAT) is illustrated in Fig. 1.1. The technique functions as follows. A number of satellites are placed in orbit around the earth so that four or more satellites always are visible from CONUS. Periodically, each satellite transmits a timing signal and accompanying data towards CONUS. The data includes satellite identification and information on the satellite location at the time of transmission. An aircraft over CONUS receives the signals by means of a top-mounted antenna with upper-hemispherical coverage. The aircraft position is determined from the signal times of arrival (TOA) using a small on-board computer. The calculated position then is displayed to the pilot as navigation information. The position also can be relayed to the ground for inclusion in the ATC data base. Thus, SAT provides navigation service and can provide (dependent) surveillance using a one-way (digital) communication link.

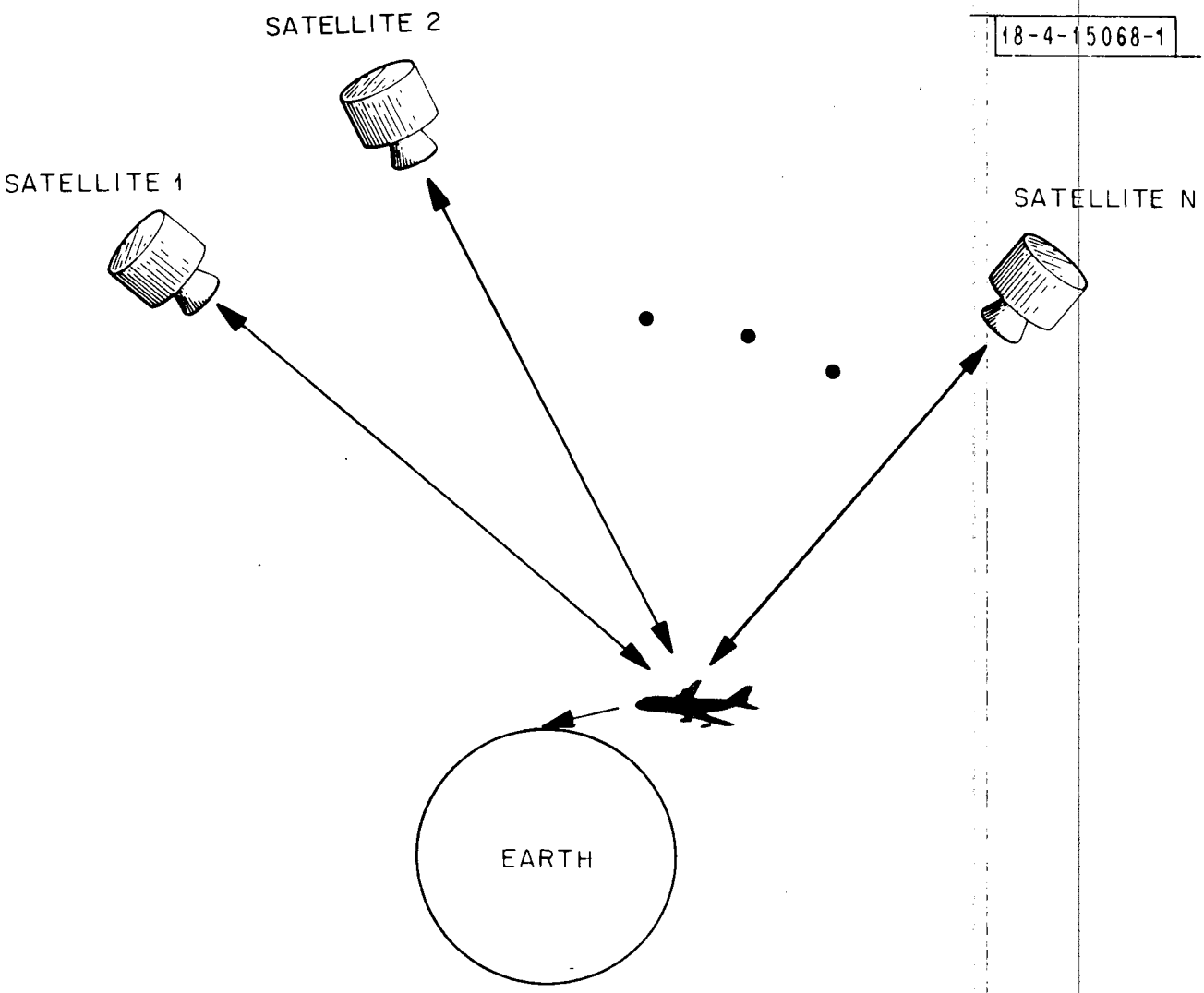

Fig. 1.1. Aircraft receives satellite signals.

1.3 PRINCIPAL CONCLUSIONS

The principal conclusions of the report are as follows.

- Development of a system employing SAT is not dependent on high risk technology.
- Navigation is the natural ATC service provided by SAT; dependent surveillance using an air-to-ground communications link is an optional service.
- Potential applications for dependent surveillance include primary surveillance in low density airspace and back-up three dimensional surveillance in high density airspace (independent of ATCRBS/DABS data).
- The on-board computing requirements are modest. While the requirements can be satisfied by a 16 bit mini-computer, they are best satisfied by a smaller special purpose computer.
- The avionics for SAT would be more costly than a present day ATCRBS transponder. The costs are closer to those of today's DME.
- Workable SAT systems can be designed that do not require a large ground-based data processing facility.
- Workable SAT systems can be designed that avoid the use of an aircraft-to-satellite uplink with its associated jamming vulnerability.

1.4 REPORT ORGANIZATION

The report examines the potential of SAT by analyzing a "baseline" system. The characteristics of the baseline system represent one data point on "the curve of characteristics obtainable from SAT." The conclusions of Section 1.3 follow from this data point, and the effort that produced it.

The report is broken into sections each of which treats a different key aspect of the baseline system. The organization is as follows:

Section II — Provides an overview of the baseline system including major engineering decisions, and functional characteristics.

Section III — Describes and analyzes the Satellite-to-Aircraft link including signalling protocol, power budget, errors due to noise, and signal format.

Section IV — Assesses the computation that must be performed on-board the aircraft.

Section V — Examines the avionics requirements both in terms of RF and digital hardware.

Section VI — Describes and analyzes some possible air to ground links.

SECTION II

THE BASELINE SYSTEM

The report explores the salient features of SAT systems through an analysis of a "baseline" system configuration. The baseline system is not intended to be a "best possible" SAT system. Instead, the intent is to provide a vehicle for examining the key technical aspects of SAT.

This section describes the key assumptions underlying the baseline system, and then gives a brief summary of the system characteristics.

2.1 BASIC ENGINEERING DECISIONS

A number of basic engineering decisions have been made in configuring the baseline system. These decisions have been strongly influenced by the need to service aircraft having moderate cost avionics, and the constraints imposed by today's technology. The main decisions are summarized below.

1. To facilitate signal detection and time of arrival estimation at the aircraft, the satellites transmit high power pulsed signals.
2. To further facilitate signal detection and estimation, the satellites utilize high-gain large-aperture antennas.
3. To prevent mutual interference among the signals at the aircraft, the satellite transmit in a round-robin sequence.
4. To simplify the avionics complement, the avionics package has only one matched filter to detect timing pulses.

2.2 MAIN CHARACTERISTICS

Care has been taken to make reasonable engineering decisions in configuring the baseline system. Nonetheless many of the decisions have been arbitrary in the sense that they have not been based upon trade-off analyses of the kind essential for system design and selection.

The main characteristics of the system are summarized in Table 2.1.

Navigation is the primary service provided by the baseline system. Navigation coverage is "down to the ground."

The system is organized so that a typical aircraft receives two complete sets of timing pulses per second. Thus, navigation updates are made twice per second.

A procedure has been developed for calculating both the aircraft position and velocity from the round robin timing pulses. Using the procedure, the avionics computer could calculate position to better than ±150 ft (rms), and velocity to better than ±20 mph (rms).

The basic avionics package consists of a top-mounted upper-hemispherical antenna, an RF receiver, and a navigation computer. As the computation requirements imposed by the position determination procedure are modest, the computer can be correspondingly modest. A suitable special purpose computer could be manufactured today at a per unit cost of approximately $1000 using conventional integrated circuits. Lower costs could be achieved by utilizing custom integrated circuits.

TABLE 2.1

CHARACTERISTICS OF THE BASELINE SYSTEM

* Down-to-the-ground navigation coverage
* Two navigation updates per second
* Air-derived position and velocity estimates
* Avionics computer less complex than a conventional mini-computer
* Extended surveillance/communications coverage by means of "austere" DABS sensors
* Compatibility with Upgraded Third Generation Air Traffic System
* No large centralized computing facility required
* Jam resistant

The baseline system also provides a surveillance service by transmitting air-derived position information to the ground. The system utilizes the DABS downlink for this purpose. The air-derived position information provides back-up surveillance data in areas already covered by DABS. Surveillance coverage can be extended to other areas by installing "austere" DABS sites. An austere DABS simply acts as a repeater interrogating aircraft in its vicinity, and relaying the reported position information to the nearest FAA center.

Use of the DABS downlink for the air-to-ground link can assure easy compatibility with the upgraded third generation air traffic system. Specifically, air-derived position information could be incorporated into the surveillance data base in a manner similar to other DABS-derived position information.

An attractive feature of the baseline system is that it does not require a large centralized computer facility to determine aircraft positions. Aircraft position is calculated in a distributed manner - each aircraft calculates its own position.

A further noteworthy feature is that the baseline system is relatively insensitive to jamming due to the absence of an air-to-satellite uplink.

SECTION III

SATELLITE-TO-AIR LINK

This section describes the satellite-to-air link of the baseline system.

The basic signaling scheme is organized so that satellites transmit in a round robin sequence. Each satellite transmission (message) includes a timing pulse, satellite identity, antenna beam identity, and satellite ephemeris data. The data accompanying the timing pulse is needed to establish the identity and position of the transmitting satellite, as well as the precise relative time of transmission.

The assumed power budget ensures a signal-to-noise ratio at the aircraft receiver sufficient to allow reliable detection and estimation of signal arrival times.

This section also discusses data formats, and correction for ionospheric delay.

3.1 SIGNALING PROTOCOL

The typical satellite-to-aircraft message for the baseline system is shown in Fig. 3.1.

The timing pulse consists of 100 DPSK encoded chips, each 500 nsec in duration, modulating a 1600 MHz carrier. The DPSK code is selected to produce a sharp "spike" suitable for timing measurements when the signal is passed through the avionics matched filter.

The data block contains information on satellite and beam identity, satellite position and velocity, and the orbital parameter ω_o^2.* Instead of transmitting complete information on position, velocity and ω_o^2, with each timing pulse the

*ω_o^2 is a parameter used to approximate satellite trajectories. (See Appendix B.)

information is transmitted piecemeal. Each 8.5 seconds enough information is transmitted to permit the on-board avionics computer to predict the satellite position and velocity over an ensuing 100 sec interval.

The data block is broken into three separate bursts to ensure that the satellite transmitter operates at a low (15%) duty cycle. Each burst is 45 μsec long and contains 9 DPSK chips representing 8 bits as shown in Fig. 3.2.

For reasons to be discussed in Section 3.2, the antenna for each satellite is assumed to have 10 beams, each covering a different portion of CONUS. Figure 3.3 illustrates how each satellite coordinates its different beams. First the message indicated in Fig. 3.1 is transmitted over Beam No. 1. Following a "dead time" of approximately 1 msec, a similar message is transmitted over Beam No. 2. After an additional 1 msec of dead time, a message is transmitted over Beam No. 3, etc. Thus, the satellite transmits the basic message over all 10 beams in 30 msec.

Provision has been made to accommodate constellations with up to 10 satellites simultaneously visible. Figure 3.4 illustrates how broadcasts from different satellites are coordinated. First, Satellite No. 1 broadcasts the sequence illustrated in Fig. 3.3. Approximately 20 msec later Satellite No. 2 broadcasts an analogous sequence, etc. Thus all satellites transmit the basic message over all beams once every half second, or twice a second.

The purpose of the 20 msec dead time is to prevent signals from different satellites from interfering at the aircraft. A signal from a satellite on the horizon requires approximately 15 msec to traverse CONUS. Thus provided the satellite broadcast times are adjusted to take account of the differeing satellite to earth transit times, the 20 msec interval is adequate to prevent interference over CONUS.

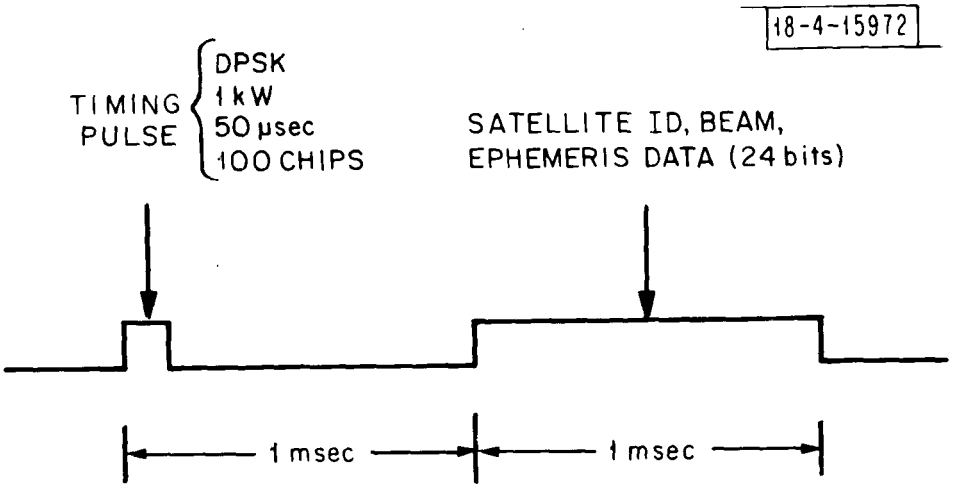

Fig. 3.1. Signal format.

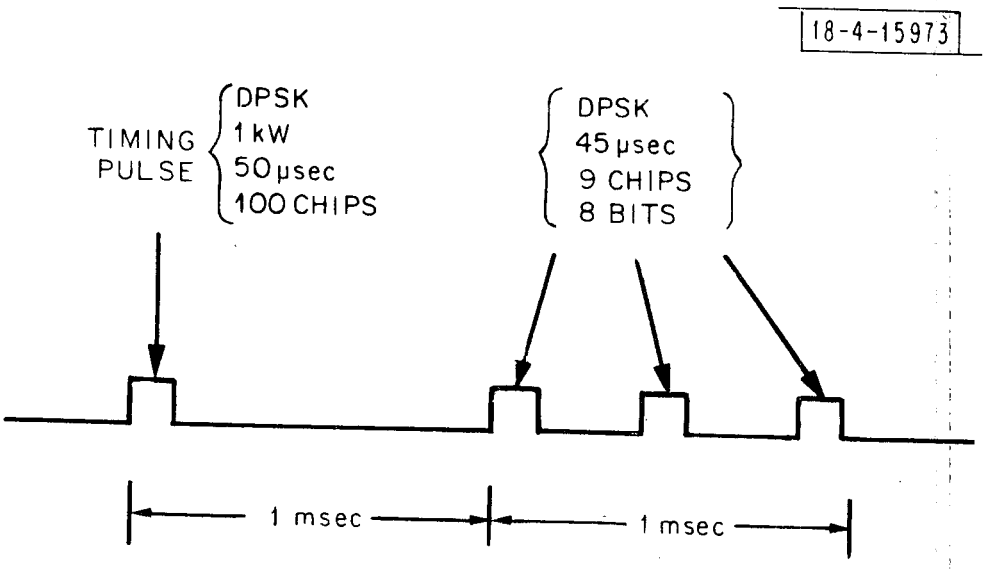

Fig. 3.2. Data block detail.

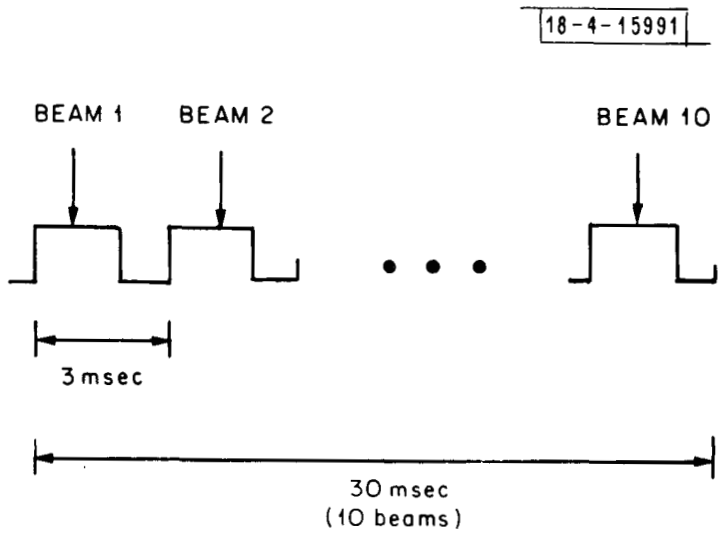

Fig. 3.3. Coordination of beam transmissions.

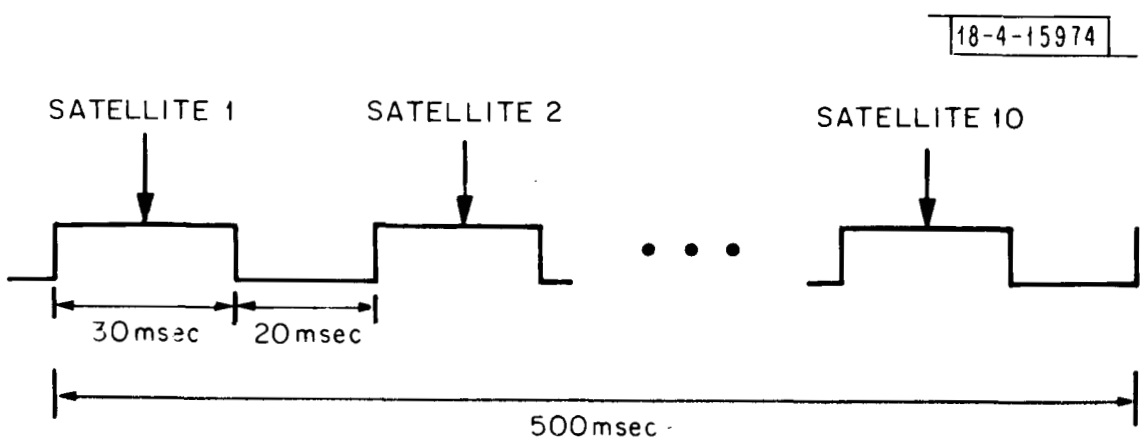

Fig. 3.4. Coordination of satellite transmissions.

3.2 POWER BUDGET

The system performance is based on the power budget of Table 3.1.

It is assumed that each satellite transmits at a peak power of 1 kW. The necessary power could be furnished by traveling wave tubes (TWT's). For example, space-qualified helix TWT's capable of 1 kW pulses of (up to) 100 μsec duration and (up to) 25% duty cycle are readily achievable.

The satellite antenna is assumed to be a large 30 ft parabolic dish like that to be deployed on ATS-F. At the assumed carrier frequency of 1.6 GHz the antenna has a narrow (1.5°) beam. Thus a single beam would cover only a portion of CONUS. Accordingly, it is assumed that the antenna has 10 separate beams which collectively cover all of CONUS. The nominal antenna gain is 42 dB. Allowances of -2 dB and -1 dB respectively are made for thermal distortion of the dish and antenna shadowing by the multiple feed structure. A further allowance of -3 dB is made for reduced antenna gain near the beam edge.

The -192 dB path loss is the worst-case loss for a satellite in a synchronous elliptical orbit of eccentricity e = 0.4.

An allowance of -1 dB is made for fading and atmospheric absorption.

Although the aircraft antenna would be designed for upper-hemispherical coverage, interactions of the antenna with the aircraft structure would preclude a completely uniform pattern. Accordingly, a minimum gain of -1 dB is assumed for elevation angles greater than 15° above the plane of the aircraft. This assumption is consistent with measurements made at (approximate) scaled frequencies.*

*See the antenna pattern on p. 54 of Ref. 12.

TABLE 3.1

SATELLITE-TO-AIRCRAFT POWER BUDGET

Transmitted Peak Power	30 dBW	1 kW
Peak Satellite Antenna Gain	42 dB	30 foot dish
Thermal Distortion	-2 dB	
Antenna Shadowing	-1 dB	
Off Boresight Loss	-3 dB	Aircraft at beam edge
Maximum Path Loss	-192 dB	Synchronous elliptical orbit, 1600 MHz
Excess Atmospheric Loss	-1 dB	
Minimum A/C Antenna Gain	-1 dB	Elevation above 15°
Received Peak Power	-128 dBW	
Received Noise Power Density	-193 dBW/Hz	3600°K, 11 dB noise figure
Received Peak Power to Noise Power Density	65 dB/sec	
Coherent Integration Time	-43 dB sec	100 - 0.5 μsec DPSK chips
Received Signal Energy to Noise Power Density	22 dB	Timing pulse signal to noise ratio

The -193 dBW/Hz noise power density corresponds to a receiver noise figure of 11 dB. Such noise figures are achievable without requiring RF pre-amplification.

The assumed avionics receiver* utilizes separate matched filters to detect the timing pulse and the data bits in Fig. 3.1. The matched filter that detects the timing pulse integrates over 50 μsec, or equivalently -43 dB sec. Thus the signal-to-noise ratio (E/N_0) at the output of the matched filter is 22 dB.

A simpler (chip) matched filter is used to detect the data bits in Fig. 3.1. The chip matched filter integrates over 5 μsec, or -53 dB sec. Therefore, the signal-to-noise ratio at the output of this filter is 12 dB.

3.3 ERRORS DUE TO NOISE

The 22 dB signal-to-noise ratio makes it possible to detect the timing pulse with high probability, and with few false alarms. For example, it is shown in Appendix A that the following performance is obtainable in the case of ideal Gaussian noise.

$$\text{Probability of Detection} \geq 1 - 1.25 \times 10^{-22}$$

$$\text{False Alarm Rate} \approx 8.4 \times 10^{-4} \text{ per day}$$

Although departures from the ideal Gaussian probability density function may change the foregoing results somewhat, the results indicate reliable detection.

The error in the measured TOA of the timing pulse due to noise can be estimated using the combined Cramer-Rao and Ziv-Zakai bounds [18]. Figure 3.5† depicts a good lower bound on the rms TOA error as a function of E/N_0 for a

*See Section 5.1.

†Taken from Ref. 18.

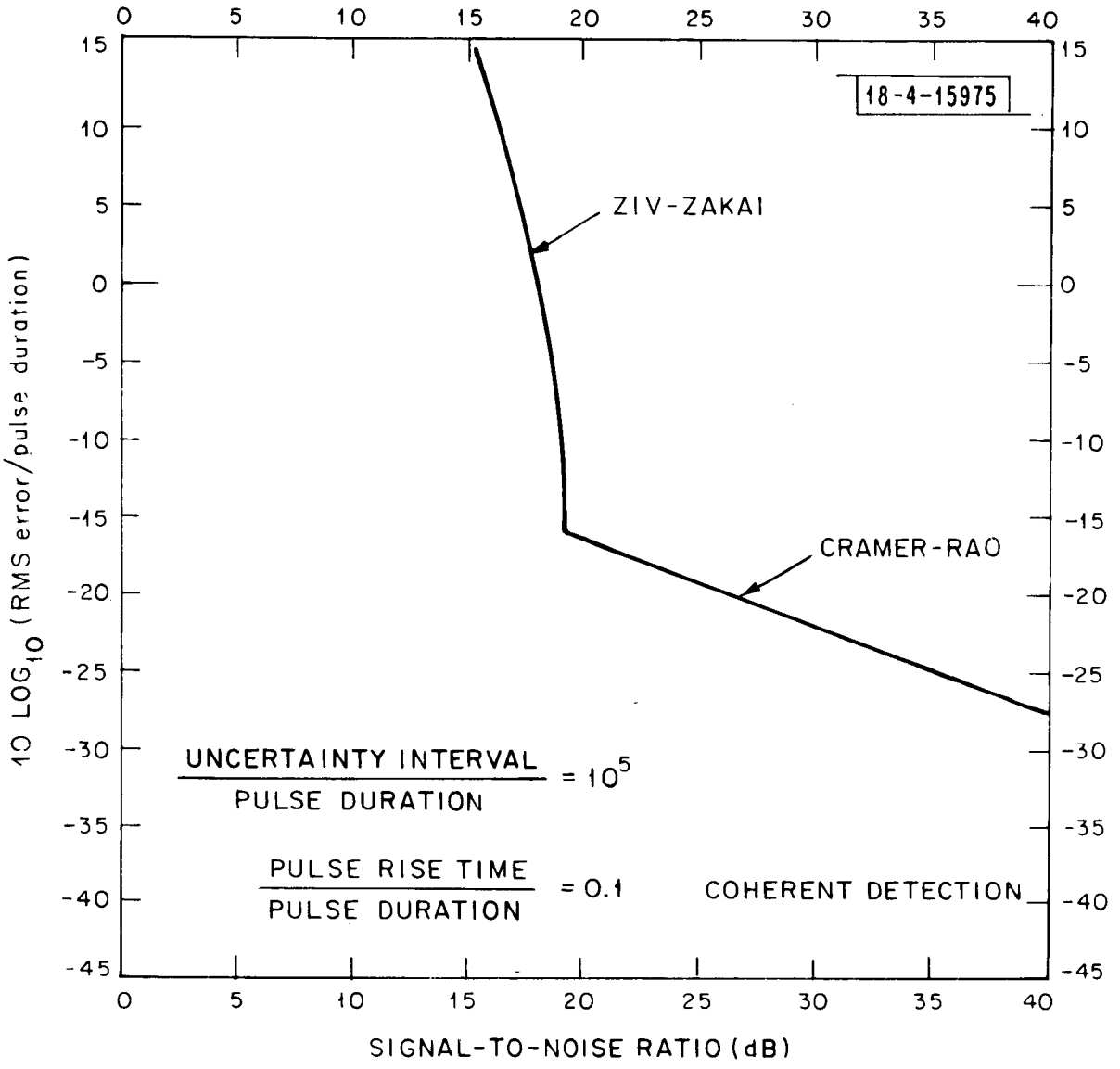

Fig. 3.5 Estimation error bounds for a trapezoidal pulse with coherent detection.

chip rise time of 50 nsec and a TOA uncertainty interval of 50 msec. It is evident from the figure that for E/N_0 = 22 dB, the TOA error is approximately

$$\text{RMS TOA Error} \approx (-17 \text{ dB})\ (500 \text{ nsec}) = 10 \text{ nsec}$$

The 12 dB signal-to-noise ratio available at the output of the chip matched filter is entirely adequate for data detection. For example, it is shown in Appendix A that the probability of bit error is smaller than 10^{-7} for ideal Gaussian noise.

3.4 DATA FORMAT

The data bits contain information on the satellite trajectory. Specifically each satellite transmits three position coordinates with one foot precision, three velocities with 0.05 ft/sec precision, and the orbital parameter ω_0^2 with a precision of one part in 10^6. The avionics computer then utilizes the data to predict the satellite position during the ensuing 100 seconds.

Table 3.2 indicates the numbers of bits required to encode the ephemeris data. A total of 170 bits is needed. Instead of transmitting the 170 bits with each timing pulse, the data is sent piecemeal. Specifically 10 of the 24 bits indicated in Fig. 3.2 are reserved for data. Thus, the ephemeris data is allocated to 17 consecutive messages. Since messages are sent at the rate of 2 per sec, a total of 8.5 sec is required to transmit complete ephemeris data.

Table 3.3 indicates how the 24 bits in each message are utilized. The first 4 bits identify the satellite transmitting the message. The next 4 bits

TABLE 3.2

DATA TO BE SENT BY EACH SATELLITE EVERY 100 SEC

3 Position Coordinates with 1 ft Accuracy	90 bits
3 Velocity Coordinates with 0.05 ft/sec Accuracy	60 bits
1 Orbital Parameter ω_o^2	20 bits
Total	170 bits

TABLE 3.3

BIT ASSIGNMENT

Bit Nos.	Function
1-4	Satellite Identity
5-8	Beam Identity
9-13	Data Type
14-23	Data
24	Parity Check

indicate the active beam.* Bits 9 through 13 specify the type of data contained in the message.† Bits 14-23 contain the data. The final bit is a parity check bit.

Since new ephemeris data is required only once every 100 sec, the ephemeris data need not be transmitted every 8.5 sec. Instead, other data (e.g., weather data) could be transmitted during the remaining 91.5 sec of every 100 sec interval.

Appendix B describes one suitable algorithm for predicting the satellite positions from the received data. The algorithm is based upon a polynomial approximation of the satellite trajectory. The predicted position is accurate to better than 10 ft over a 100 sec interval given data of the indicated accuracy.

3.5 PRE-CORRECTION FOR IONOSPHERIC DELAY

The ionosphere typically delays downlink signals by times ranging from 4 nsec to 40 nsec. The uncertainty as to the actual delay contributes significantly to the error in the final position estimate.

SAT provides a simple mechanism for pre-correcting such delay. Specifically the ionospheric delay can be measured by a network of ground calibration stations. The downlink transmissions then can be advanced to offset the measured delays. For purposes of the baseline system it is assumed that the signal transmission times are advanced in this manner. Note that this refinement causes the signal transmission times to depart slightly from the equal spacing indicated in Fig. 3.3.‡

*Needed to establish the transmission time of the timing pulse.

†That is, the ephemeris parameter to which the data relates. Also whether the data represents the first, second or third 10 bits of the parameter.

‡Since different beams are advanced by different time increments.

SECTION IV

ON-BOARD COMPUTING REQUIREMENTS

An aircraft over CONUS always is within one or more beams from each satellite. Thus as the satellites broadcast in their round robin sequence, the aircraft receives a sequence of timing pulses like that shown in Fig. 4.1. The problem that must be solved in the on-board computer is that of calculating the aircraft position from the signal TOA's. This amounts to solving a set of TOA equations.

Note that the position determination problem for RAST and CAST is different from that just described. In RAST and CAST the aircraft transmits a single pulse which is received by the satellites at different times. Thus the aircraft position is the same for all received pulses. By contrast in the baseline SAT system the pulse transmission times are staggered. Thus the aircraft position changes from pulse to pulse, which complicates the position determination problem.*

This section examines the problem of calculating the aircraft position, given that the timing pulses are sent sequentially rather than simultaneously. Ideally a suitable computational procedure would combine the following attributes.

1. The procedure is sufficiently simple that it can be programmed on a mini-computer.
2. The procedure provides an accurate indication of aircraft position in spite of the fact that position is changing while the data is being collected.

The primary conclusion of the chapter is that such procedures do exist.

*This complication is the price of avoiding the problems associated with signal overlap at the aircraft (e.g., mutual interference, multiple matched filters).

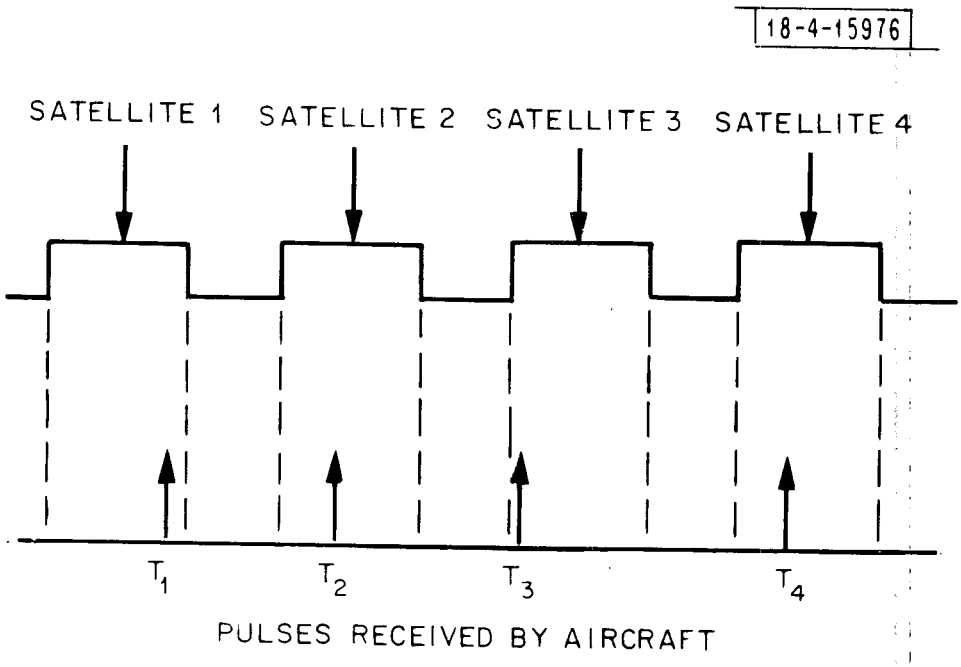

Fig. 4.1. Timing pulses received by aircraft.

The position determination procedure that first suggests itself is conventional hyperbolic multilateration. While comparatively simple from a computational point of view, this procedure ignores aircraft motion between timing pulses. Thus the procedure makes a "motional error" in addition to the normal positional error. For aircraft flying at General Aviation speeds the motional error is shown to be negligible compared to other sources of error. By contrast, for aircraft flying at Air Carrier speeds "motional error" exceeds all other errors. Accordingly, hyperbolic multilateration is not used in the baseline system.

The next procedure considered takes account of aircraft motion by assuming it to be constant velocity motion along a straight line. The procedure sequentially calculates the straight line trajectory that best fits the TOA data in a least squares sense. The squared TOA errors are weighted by an exponential factor with time constant τ to emphasize recent data and de-emphasize old. On the one hand, the procedure is reasonable from a computational point of view. On the other hand, the procedure produces ATC quality accuracies provided τ is properly chosen. Accordingly the procedure is selected for use in the baseline design.

4.1 THE POSITION DETERMINATION PROBLEM

All procedures for determining the position of the aircraft are procedures for solving the TOA equations.

The ideal TOA equations are as follows:

$$\begin{aligned} \tau_1 &= T_1 + d_1/c + \varepsilon_1 \\ \tau_2 &= T_2 + d_2/c + \varepsilon_2 \\ \tau_k &= T_k + d_k/c + \varepsilon_k \end{aligned} \tag{4.1.1}$$

where

τ_j = The arrival time of the j^{th} pulse.

T_j = The transmission time of the j^{th} pulse.

d_j = The distance between the j^{th} satellite at time T_j and the aircraft at time τ_j.

d_j/c = The transit time of the pulse from the j^{th} satellite to the aircraft.

ε_j = The effective error in the TOA of the j^{th} pulse due to satellite position inaccuracies, atmospheric disturbances, and receiver noise.

Presumably the precise times T_j of signal transmission are unknown, but the interpulse intervals are precisely known. Thus it is convenient to set

$$T_j = T_0 + \sum_{i=1}^{j} \Delta\tau_{i-1,i} \tag{4.1.2}$$

where

$\Delta\tau_{i-1,i}$ = The known time interval between transmission of the (i-1)th and the i^{th} pulses.

T_0 = An unknown reference time.

With this understanding Eq. (4.1.1) can be rewritten,

$$\begin{aligned}
\tau_1 - \Delta\tau_{01} &= T_o + d_1/c + \varepsilon_1 \\
\tau_2 - \sum_{i=1}^{2} \Delta\tau_{i-1,i} &= T_0 + d_2/c + \varepsilon_2 \\
&\vdots \\
\tau_k - \sum_{i=1}^{k} \Delta\tau_{i-1,i} &= T_0 + d_k/c + \varepsilon_k
\end{aligned} \tag{4.1.3}$$

where all of the knowns have been placed to the left of the equal signs.

On the surface, Eqs. (4.1.3) appear to be linear. However, the equations become non-linear when the distanced d_j are expressed in terms of any convenient coordinate system. For example, d_j takes the following form when expressed in terms of Cartesian coordinates

$$d_j = \sqrt{(x - x_j)^2 + (y - y_j)^2 + (z - z_j)^2} \tag{4.1.4}$$

Thus for purposes of solving Eq. (4.1.3) it is advantageous to linearize the d_j about a reference point near the aircraft, and then solve the equations for the aircraft location relative to the reference point. To first order d_j can be expressed as follows:

$$d_j = r_j + \underline{i}_j \cdot \underline{\Delta r}_j \tag{4.1.5}$$

where

r_j = The distance between the j^{th} satellite and the reference point at time T_j.

$\underline{i}_j$ = A (1x3) unit vector pointing from the aircraft to the satellite (see Fig. 4.2).

$\underline{\Delta r}_j$ A (3x1) vector specifying the location of the aircraft relative to the reference point (see Fig. 4.2). It is assumed that the elements of $\underline{\Delta r}_j$ are expressed in terms of a conveniently chosen cartesian coordinate system centered at the reference point.

With the approximation of Eq. (4.1.5), Eqs. (4.1.3) can be rewritten

$$\begin{aligned}
(c\tau_1 - c\,\Delta\tau_{01} - r_1) &= cT_0 + \underline{i}_1 \cdot \underline{\Delta r}_1 + c\,\varepsilon_1 \\
(c\tau_2 - c\sum_{i=1}^{2}\Delta\tau_{i-1,1} - r_2) &= cT_0 + \underline{i}_2 \cdot \underline{\Delta r}_2 + c\,\varepsilon_2 \\
&\vdots \\
(c\tau_k - c\sum_{i=1}^{k}\Delta\tau_{i-1,i} - r_k) &= cT_0 + \underline{i}_k \cdot \underline{\Delta r}_k + c\,\varepsilon_k
\end{aligned} \tag{4.1.6}$$

where again all knowns have been placed to the left of the equal signs.

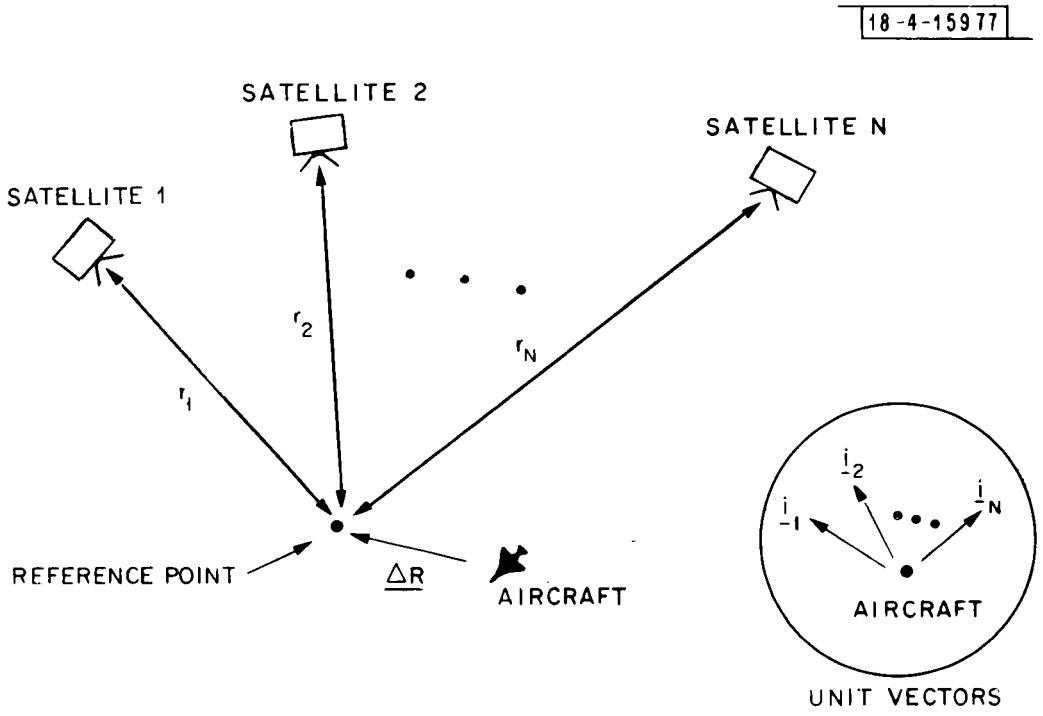

Fig. 4.2. Illustrating linearization of TOA equations.

Ignoring for the moment the errors ε_j, the system of Eq. (4.1.6) is underdetermined in that it consists of k equations in 3k+1 unknowns, the unknowns being the three elements of each of the $\underline{\Delta r}_j$, and the time T_0. Thus to solve Eq. (4.1.6) it is necessary to reduce the number of unknowns. This can be done by making assumptions about the aircraft trajectory. Two different assumptions are considered here. The assumptions are as follows.

1. Aircraft motion is negligible during one complete sequence of timing pulses. That is

$$\underline{\Delta r}_1 = \underline{\Delta r}_2 \cdots = \underline{\Delta r}_k = \underline{X} \quad . \tag{4.1.7}$$

2. The aircraft moves at constant velocity along a straight line trajectory. That is

$$\underline{\Delta r}_j = \underline{X} + \dot{\underline{X}}(\tau_j - \tau_k) \tag{4.1.8}$$

where

$\underline{X}$ = A (3x1) vector specifying the aircraft location at time τ_k.

$\dot{\underline{X}}$ = The (3x1) aircraft velocity vector.

The assumption (4.1.7) reduces Eq. (4.1.6) to a system of k equations in 4 unknowns which is determinate (or over determined) provided $k \geq 4$.

The assumption (4.1.8) reduces Eq. (4.1.6) to a system of k equations in seven unknowns which is determinate (or over determined) provided $k \geq 7$.

4.2 TOA ERROR ASSUMPTIONS

The TOA errors are primarily due to ionospheric delay, uncertainties in satellite position, and receiver noise. It is assumed that the mean ionospheric delay has been removed from the TOAs $\tau_1, \tau_2, \ldots, \tau_k$ by the method described in Section 3.5. Thus the ε_j in Eq. (4.1.1) represent the residual ionospheric delay, uncertainties in satellite position, and errors due to receiver noise.

For present purposes the ε_j are modelled as uncorrelated random variables having variances of $\sigma_1^2, \sigma_2^2, \ldots, \sigma_k^2$. That is, it is assumed that the ε_j have a diagonal covariance matrix as follows:

$$\underline{P}_k = \begin{bmatrix} \sigma_1^2 & & \text{O} \\ & \sigma_2^2 & \\ & & \ddots \\ \text{O} & & & \sigma_k^2 \end{bmatrix} \qquad (4.2.1)$$

4.3 IGNORING AIRCRAFT MOTION

From a computational point of view, the simplest method of determining (estimating) aircraft position is to ignore aircraft motion, and solve Eq. (4.1.6) for the aircraft position once every (1/2 second) timing cycle.

This approach amounts to solving the system of Eq. (4.1.6) with the assumption Eq. (4.1.7), or equivalently to solving the equations

$$
\begin{aligned}
(c\tau_1 - c\Delta\tau_{01} - r_1) &= (c\,T_0) + \underline{i}_1 \cdot \underline{X} + c\,\varepsilon_1 \\
(c\tau_2 - c\sum_{i=1}^{2} \Delta\tau_{i-1,i} - r_2) &= (c\,T_0) + \underline{i}_2 \cdot \underline{X} + c\,\varepsilon_2 \\
&\vdots \\
(c\tau_k - c\sum_{i=1}^{k} \Delta\tau_{i-1,i} - r_k) &= (c\,T_0) + \underline{i}_k \cdot \underline{X} + c\,\varepsilon_k
\end{aligned}
\tag{4.3.1}
$$

It is convenient to condense the system Eq. (4.3.1) into a single matrix equation as follows

$$
\underline{K}_k = (cT_0)\,\underline{1} + \underline{F}_k\,\underline{X} + c\,\underline{\varepsilon}_k \tag{4.3.2}
$$

where

$$
\underline{K}_k = \begin{bmatrix}
(c\tau_1 - c\Delta\tau_{01} - r_1) \\
(c\tau_2 - c\sum_{i=1}^{2} \Delta\tau_{i-1,i} - r_2) \\
\vdots \\
(c\tau_k - c\sum_{i=1}^{k} \Delta\tau_{i-1,i} - r_k)
\end{bmatrix}
\tag{4.3.3}
$$

and

$$
\underline{1} = \left.\begin{bmatrix} 1 \\ 1 \\ \vdots \\ 1 \end{bmatrix}\right\} k \text{ rows}
\tag{4.3.4}
$$

$$\underline{F}_k = \underbrace{\left[\begin{bmatrix} \underline{i}_1 \\ \underline{i}_2 \\ \vdots \\ \underline{i}_k \end{bmatrix}\right.}_{3 \text{ columns}} \left.\vphantom{\begin{bmatrix} \underline{i}_1 \\ \underline{i}_2 \\ \vdots \\ \underline{i}_k \end{bmatrix}}\right\} k \text{ rows} \tag{4.3.5}$$

$$\underline{\varepsilon}_k = \begin{bmatrix} \varepsilon_1 \\ \varepsilon_2 \\ \cdot \\ \cdot \\ \varepsilon_k \end{bmatrix} \tag{4.3.6}$$

The least squares solution of Eq. (4.3.2) is as follows

$$\underline{\hat{X}} = [\underline{F}_k' \, \underline{Q}_k \, \underline{F}_k]^{-1} \, \underline{F}_k' \, \underline{Q}_k \, \underline{K}_k \tag{4.3.7}$$

where

$$\underline{Q}_k = \underline{P}_k^{-1} - \frac{1}{(\underline{1}' \, \underline{P}_k^{-1} \, \underline{1})} \, \underline{P}_k^{-1} \, \underline{1} \, \underline{1}' \underline{P}_k^{-1} \tag{4.3.8}$$

(See Appendix C.1 for a derivation.)

Whether the estimate (4.3.7) is acceptable from a performance point of view depends upon the "motional error," or the error in the calculated position that results from ignoring aircraft motion.

For the purpose of assessing motional error, the following simplifying assumptions are made.

1. Successive TOA's differ by a uniform increment ΔT. That is

$$\tau_j = \tau_k - (k - j)\,\Delta T \tag{4.3.9}$$

2. During the time interval in which pulses 1,2...,k are collected, the aircraft flies at a constant velocity in a straight line. That is

$$\underline{X}_{\tau j} = \underline{X}_{\tau k} - (k - j)\,\Delta T\,\dot{\underline{X}} \tag{4.3.10}$$

where $\underline{X}_{\tau j}$ specifies the vector location at time τ_j, and $\dot{\underline{X}}$ is the vector velocity.

3. All other sources of error are zero. That is

$$\varepsilon_j = 0 \tag{4.3.11}$$

With these assumptions, the arrival times are as follows

$$\tau_1 = T_o + \Delta\tau_{01} + \frac{r_1}{c} + \frac{1}{c}\,\underline{i}_1 \cdot \underline{X} - \frac{1}{c}(k-1)\Delta T\;\underline{i}_1 \cdot \dot{\underline{X}}$$

$$\tau_2 = T_o + \sum_{j=1}^{2} \Delta\tau_{j-1,j} + \frac{r_2}{c} + \frac{1}{c}\,\underline{i}_2 \cdot \underline{X} - \frac{1}{c}(k-2)\Delta T\,\underline{i}_2 \cdot \dot{\underline{X}}$$

$$\vdots$$

$$\tau_k = T_o + \sum_{j=1}^{k} \Delta\tau_{j-1,j} + \frac{r_k}{c} + \frac{1}{c}\,\underline{i}_k \cdot \underline{X} \qquad (4.3.12)$$

Use of the arrival times (4.3.12) in the vector (4.3.3) and use of the result in (4.3.7) produces the following expression for the motional error

$$\hat{\underline{X}}_{\tau k} - \underline{X}_{\tau k} = -\Delta T\,[\underline{F}_k'\,\underline{Q}_k\,\underline{F}_k]^{-1}\;\underline{F}'\,\underline{Q}_k\,\underline{S}_k\,\underline{F}\,\dot{\underline{X}} \qquad (4.3.13)$$

where $\underline{S}_k$ is the diagonal matrix

$$\underline{S}_k = \begin{bmatrix} (k-1) & & & \\ & (k-2) & & \\ & & \ddots & \\ & & & 1 \\ & & & 0 \end{bmatrix} \qquad (4.3.14)$$

The following properties of motional error are apparent from (4.3.13)

1. Motional error is directly proportional to the interpulse interval ΔT. Thus, for example, halving the signaling rate doubles the motional error.

2. Motional error is directly proportional to velocity. Thus doubling velocity doubles the motional error.

3. Nearby aircraft flying in opposite directions have oppositely directed error vectors. [This follows since all matrix factors in (4.3.13) are identical for both aircraft except for the velocity vectors, which are negatives.]

4. Motional error depends on the signaling sequence, or the order in which the satellites transmit. [This follows since changing the signaling sequence permutes the rows of (4.3.5) and also the rows and columns of (4.3.8) and consequently, changes (4.3.13)].

In Appendix C.2 it is shown that if (4.3.13) is averaged over all possible signaling sequences, the mean error is given by

$$E[\hat{\underline{X}}_{\tau k} - \underline{X}_{\tau k}] = -\frac{(k-1)\,\Delta T}{2}\,\dot{\underline{X}} \qquad (4.3.15)$$

Thus "on the average" the estimate (4.3.7) calculates the "halfway point" of the aircraft trajectory over the interval (τ_1, τ_k).

Clearly if (4.3.7) were approximately to calculate the "halfway point" for every signaling sequence, then (4.3.7) would be a highly useful estimate. For the estimate would provide an accurate altitude indication, since

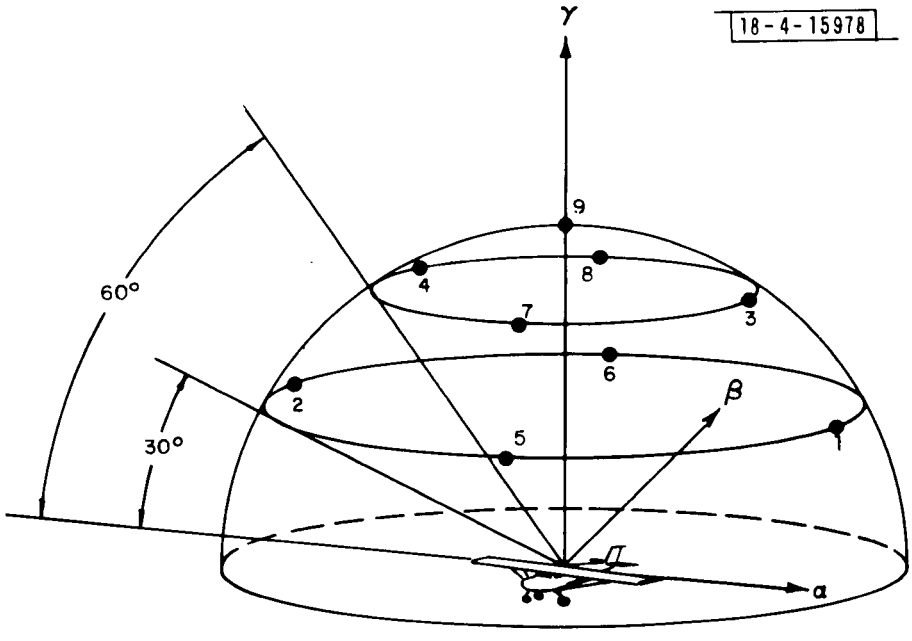

Fig. 4.3. Representative constellation.

altitude is essentially constant over one signaling interval (τ_1, τ_k). Moreover, successive position estimates could be used to generate a velocity estimate which then could be used to correct $\hat{\underline{X}}$ for the error (4.3.15).

Expressions are derived in Appendix C.2 for the rms deviation of the estimate (4.3.7) from the "halfway point". When specialized to the representative satellite deployment shown in Fig. 4.3, and an aircraft traveling at constant velocity V_α in the α-direction, the results take the following form.

$$\sigma_\alpha = 1.231\ (V_\alpha \Delta\tau) \tag{4.3.16}$$

$$\sigma_\beta = 0 \tag{4.3.17}$$

$$\sigma_\delta = 2.201\ (V_\alpha \Delta\tau) \tag{4.3.18}$$

For a velocity of V_α = 150 mph (220 fps) and the interpulse spacing of $\Delta\tau$ = 0.05 sec described in Section 3.1,

$$\sigma_\alpha = 13.5 \text{ ft} \tag{4.3.19}$$

$$\sigma_\beta = 0 \text{ ft} \tag{4.3.20}$$

$$\sigma_\delta = 24.2 \text{ ft} \tag{4.3.21}$$

For a velocity V_α = 650 mph, and $\Delta\tau$ = 0.05 sec

$$\sigma_\alpha = 58.5 \text{ ft} \tag{4.3.22}$$

$$\sigma_\beta = 0 \text{ ft} \tag{4.3.23}$$

$$\sigma_\delta = 104.9 \text{ ft} \tag{4.3.24}$$

The errors (4.3.19)-(4.3.21) are comparable to the errors due to other sources (e.g., ionospheric delay, receiver noise, clock error). Thus motional error is not significant for aircraft moving at speeds typical of General Aviation aircraft. Even if the signaling rate is halved (or $\Delta\tau$ doubled), the resulting errors are not excessive.

By contrast, the error (4.3.24) is larger than the errors due to other sources. Moreover the error is aggravated by the fact that oppositely directed aircraft have oppositely directed error vectors. Thus, for example, it is possible for an east-bound and west-bound aircraft to be on a collision course at 6,750 ft with the instruments aboard the east-bound aircraft indicating a safe altitude of 7,000 ft and those aboard the west-bound aircraft indicating a safe 6,500 ft altitude. In both cases the aircraft make (2.5σ) motional errors of 250 ft. The error made by the east-bound aircraft is +250 ft while that made by the west-bound aircraft is -250 ft. Thus motional errors assume serious magnitudes for aircraft traveling at air carrier speeds. Decreasing the signaling rate worsens the problem.

Presumably an operational satellite system must provide comparable safe service to both general aviation and air carrier aircraft. Accordingly, conventional hyperbolic multilateration is not used in the baseline system.

4.4 CONSTANT VELOCITY MOTION

Aircraft motion is accounted for by assuming the constant velocity straight line trajectory of Eq. (4.1.8). Substitution of Eq. (4.1.8) in Eq. (4.1.6) gives

$$
\begin{aligned}
(c\tau_1 - c\Delta\tau_{01} - r_1) &= cT_0 + \underline{i}_1 \cdot \underline{X} + (\tau_1 - \tau_k)\,\underline{i}_1 \cdot \dot{\underline{X}} + c\,\varepsilon_1 \\
\left(c\tau_2 - c\sum_{i=1}^{2}\Delta\tau_{i-1,i} - r_2\right) &= cT_0 + \underline{i}_2 \cdot \underline{X} + (\tau_2 - \tau_k)\,\underline{i}_2 \cdot \dot{\underline{X}} + c\,\varepsilon_2 \\
&\vdots \\
\left(c\tau_k - c\sum_{i=1}^{k}\Delta\tau_{i-1,i} - r_k\right) &= cT_0 + \underline{i}_k \cdot \underline{X} + (\tau_k - \tau_k)\,\underline{i}_k \cdot \dot{\underline{X}} + c\,\varepsilon_k
\end{aligned}
\tag{4.4.1}
$$

It is convenient to condense Eq. (4.4.1) as follows using matrix notation

$$
\underline{K}_k = (cT_0)\,\underline{1} + \underline{N}_k\,\underline{X} + c\,\underline{\varepsilon}_k \tag{4.4.2}
$$

where the vectors $\underline{K}_k$, $\underline{1}$ and $\underline{\varepsilon}_k$ are as in Section 4.3 and

$$
\underline{X} = \begin{bmatrix} \underline{X} \\ -- \\ \dot{\underline{X}} \end{bmatrix} \quad (6 \times 1), \qquad
\underline{N}_k = \begin{bmatrix} \underline{i}_1 & (\tau_1 - \tau_k)\underline{i}_1 \\ \underline{i}_2 & (\tau_2 - \tau_k)\underline{i}_2 \\ \vdots & \vdots \\ \underline{i}_k & (\tau_k - \tau_k)\underline{i}_k \end{bmatrix} \quad (k \times 6)
\tag{4.4.3-4}
$$

One method of determining (estimating) the position and velocity subvectors $\underline{X}$ and $\dot{\underline{X}}$ is to collect data for $n \geq 7$ timing pulses so that the system (4.4.1) is determinate (or over determined), and then solve for $\underline{X}$ using the least squares method. This approach produces a position update once every n timing pulses.

An alternate approach is employed here because it leads to an attractive computer realization. The method produces the same estimate as would be obtained by solving the entire system of Eq. (4.4.1). The method is formulated in a sequential manner, however. Thus each new state vector $\hat{\underline{X}}_k$ is calculated from the previous state vector $\hat{\underline{X}}_{k-1}$ and the new data, rather than by re-solving the (growing) system of Eqs. (4.4.1). A side benefit of the method is that it provides a new position update after every timing pulse, as opposed to once every n pulses.

Provision is made for departure of the aircraft from the assumed straight line trajectory by exponentially weighting the errors in the application of the least squares principle. Specifically, after each timing pulse, the vector $\underline{X}$ that minimizes the error measure

$$E_k = \sum_{i=1}^{k} e^{-(\tau_k - \tau_i)/\tau} (\varepsilon_i/\sigma_i)^2 \qquad (4.4.5)$$

is selected as the "solution" of Eq. (4.4.2). The exponential weighting factor is illustrated in Fig. 4.4. By weighting recent errors more heavily than old errors, the method emphasizes new data and de-emphasizes old. Thus in effect the method solves the subset of Eqs. (4.4.1) that fall within a "calculation

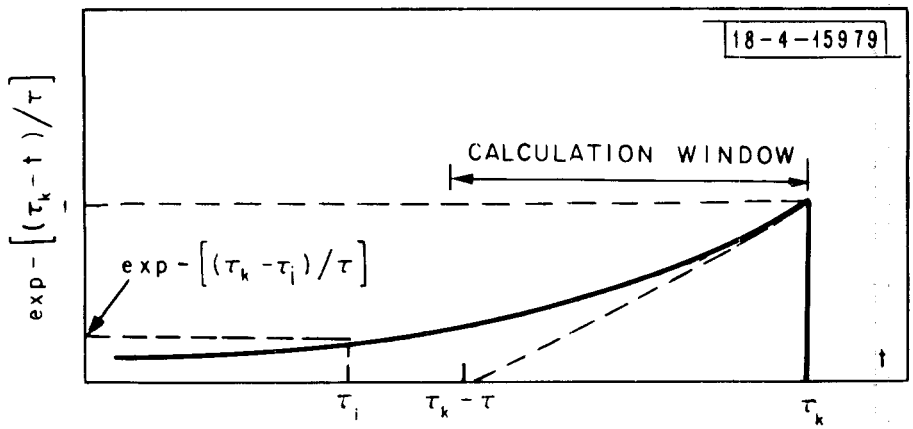

Fig. 4.4. Exponential weighting function.

window" corresponding to the most recent τ seconds. Proper pre-selection of τ ensures that aircraft maneuvers can be tracked.

The details of the solution are deferred to Appendix C.3. The resulting equation for generating the new state vector $\underline{\chi}_k$ is as follows

$$\hat{\underline{\chi}}_k = \underline{M}_k^{-1} \hat{\underline{\chi}}_{k-1} + \frac{1}{d_k} \underline{\Lambda}_k \underline{a}_k'(y_k - \underline{a}_k \underline{M}_k^{-1} \hat{\underline{\chi}}_{k-1}) \quad . \tag{4.4.6}$$

The quantities $\underline{M}_k^{-1}$, d_k, $\underline{\Lambda}_k$, $\underline{a}_k$ and y_k are defined in Appendix C.3. The matrix $\underline{M}_k^{-1}$ serves to "advance" the old state vector $\hat{\underline{\chi}}_{k-1}$ along a straight line trajectory. That is

$$\underline{M}_k^{-1} \hat{\underline{\chi}}_{k-1} = \begin{bmatrix} \hat{\underline{\chi}}_{k-1} + (\tau_k - \tau_{k-1}) \dot{\hat{\underline{\chi}}}_{k-1} \\ \hline \dot{\hat{\underline{\chi}}}_{k-1} \end{bmatrix} \tag{4.4.7}$$

Thus (4.4.6) updates the state vector $\underline{\chi}$ in the following steps:

1. The preceding state vector $\hat{\underline{\chi}}_{k-1}$ is advanced according to Eq. (4.4.7).
2. The correction term $\frac{1}{d_k} \underline{\Lambda}_k \underline{a}_k'(y_k - \underline{a}_k \underline{M}_k^{-1} \hat{\underline{\chi}}_{k-1})$ is added to the result.

The accuracy of the method for flight conforming to the straight line trajectory (4.1.8) can be assessed by examining the covariance matrices for position and velocity errors. Accordingly, bounds were developed for the covariance matrices subject to the following conditions.

1. N (visible) satellites periodically transmit timing pulses.
2. The transmission times are staggered so that the typical aircraft receives a complete set of timing pulses once every T seconds.

For $\tau >> T$ and $\tau_k >> \tau$ the bounds take the following form*†

Position:

$$E[(\hat{\underline{X}} - \underline{X})(\hat{\underline{X}} - \underline{X})'] \leq \frac{T}{\tau} c^2 [(\underline{F}_N' \underline{Q}_N \underline{F}_N)^{-1} + (\underline{F}_N' \underline{P}_N^{-1} \underline{F}_N)^{-1}] \quad (4.4.8)$$

Velocity:

$$E[(\hat{\dot{\underline{X}}} - \dot{\underline{X}})(\hat{\dot{\underline{X}}} - \dot{\underline{X}})'] \leq \frac{T}{\tau^3} c^2 (\underline{F}_N' \underline{P}_N^{-1} \underline{F}_N)^{-1} \quad (4.4.9)$$

where $\underline{F}_N$, $\underline{Q}_N$ and $\underline{P}_N$ denote the matrices (4.3.5), (4.3.8) and (4.2.1) evaluated for k=N, and c denotes the velocity of light. Thus, for example, if

$$\sigma_1^2 = \sigma_2^2 = \ldots = \sigma_9^2 = \sigma^2 \quad (4.4.10)$$

the covariance matrices for the satellite deployment of Figure 4.3

*The condition $\tau >> T$ means that the calculation window extends over several signaling periods. The condition $\tau_k >> \tau$ means that several time constants have elapsed (so that the covariance matrices have settled to steady state values).

†The notation $\underline{A} \leq \underline{B}$ for matrices $\underline{A}$ and $\underline{B}$ as used here means that $\underline{\zeta}' \underline{A} \underline{\zeta} \leq \underline{\zeta}' \underline{B} \underline{\zeta}$ for any vector $\underline{\zeta}$.

are bounded as follows

Position:

$$E[(\hat{\underline{X}} - \underline{X})((\hat{\underline{X}} - \underline{X})'] \leq \frac{T}{\tau}(\sigma c)^2 \begin{bmatrix} 1 & 0 & 0 \\ 0 & 1 & 0 \\ 0 & 0 & 3 \end{bmatrix} \qquad (4.4.11)$$

Velocity:

$$E[(\hat{\dot{\underline{X}}} - \dot{\underline{X}})\ (\underline{X} - \dot{\underline{X}})'] \leq \frac{T}{\tau^3}(\sigma c)^2 \begin{bmatrix} 0.5 & 0 & 0 \\ 0 & 0.5 & 0 \\ 0 & 0 & 0.2 \end{bmatrix} \qquad (4.4.12)$$

For the values

$$T = 0.5 \text{ sec}$$
$$\tau = 2 \text{ sec}$$
$$(\sigma c) = 50 \text{ ft} \qquad (4.4.13\text{-}15)$$

the rms position and velocity errors are bounded as follows

$$\sigma_\alpha = \sigma_\beta \leq 25 \text{ ft}$$
$$\sigma_\gamma \leq 43.3 \text{ ft}$$
$$\sigma_{TOT} \leq 55.9 \text{ ft} \qquad (4.4.16\text{-}18)$$

$$\sigma_{\dot{\alpha}} = \sigma_{\dot{\beta}} \leq 6 \text{ mph}$$
$$\sigma_{\dot{\gamma}} \leq 3.8 \text{ mph}$$
$$\sigma_{\dot{X}} = \left[\sigma_{\dot{\alpha}}^2 + \sigma_{\dot{\beta}}^2 + \sigma_{\dot{\alpha}}^2\right]^{1/2} = 9.3 \text{ mph} \qquad (4.4.19\text{-}21)$$

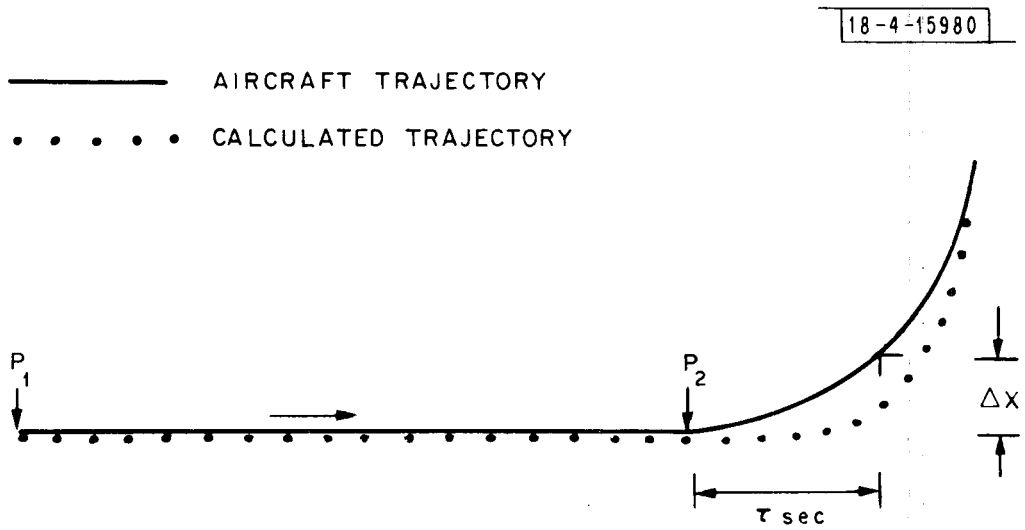

Fig. 4.5. Assessment of maneuvers error.

Clearly, the position errors of Eq. (4.4.16-18) represent an improvement over those for the method of Section 4.3 [see Eqs. 4.3.22-24]. By increasing the time constant τ the errors can be further reduced. This reduction results from the fact that redundant data is available within the calculation window permitting cancellation of errors. Note that as τ is increased velocity errors decrease more rapidly than position errors.

The accuracy of the method during maneuvers cannot be assessed so easily. A hueristic understanding of the impact of maneuvers can be gained as follows, however. Assume that an aircraft travels at a constant velocity V along the trajectory shown in Fig. 4.5. That is, the aircraft flies a straight line course from Point 1 to Point 2. At Point 2 the aircraft begins to change heading at the rate of dh/dt degrees per second. Clearly, for a short time after the aircraft begins to turn, most of the data contained within the "calculation window" corresponds to the earlier straight line flight. As the algorithm produces a "best" straight line fit to this data, it continues to project straight line flight as indicated in Fig. 4.5. After a time τ, however, the data within the calculation window becomes primarily curved flight data. At this point the algorithm begins tracking the curve as shown. Thus it is reasonable to expect that the method makes an error corresponding to the distance Δx in Fig. 4.5. A straightforward calculation shows that

$$\Delta x \approx \frac{\pi V \tau^2}{360} \frac{dh}{d\tau} \quad . \tag{4.4.22}$$

For the values

$$V = 300 \text{ mph} \tag{4.4.23}$$

$$\frac{dh}{dt} = 3 \text{ deg/sec} \tag{4.4.24}$$

$$\tau = 5 \text{ sec} \tag{4.4.25}$$

the "maneuvers error" is

$$\Delta x \approx 11.52\ \tau^2$$
$$= 288 \text{ ft} \tag{4.4.26}$$

Comparison of Eq. (4.4.11) and Eq. (4.4.22) shows that the dual objectives of accuracy during straight line flight and accuracy during maneuvers place conflicting demands on the parameter τ. High accuracy during straight line flight calls for a large value of τ. By contrast, accuracy during maneuvers calls for a small value of τ. For present purposes, the value

$$\tau = 2 \text{ sec} \tag{4.4.27}$$

represents a reasonable compromise, and is the value used in the baseline design. The associated position and velocity errors for straight line flight are those given in Eqs. (4.4.16-21). For the values

$$V = 300 \text{ mph} \tag{4.4.28}$$

$$\frac{dh}{dt} = 3 \text{ deg/sec} \tag{4.4.29}$$

the corresponding maneuvers error (4.4.22) is

$$\Delta x = 46 \text{ ft} \tag{4.4.30}$$

4.5 COMPUTATIONAL REQUIREMENTS

A flow chart for calculating $\underline{\chi}_k$ is given in Fig. 4.6. The individual operations are explained in Appendix C.3.

The computational requirements for updating $\underline{\chi}_k$ are summarized in Table 4.1. Each row of the table indicates the requirements imposed by the corresponding box of the flow chart.

Note that if each floating point operation consumes 10 μsec, then the position update requires approximately 4 msec. Thus the twenty updates per second described in Section 3.1 require $20 \times 4 \approx 80$ msec of processor time per second, or 8% of the processor capacity.

TABLE 4.1

COMPUTATIONAL REQUIREMENTS FOR UPDATING $\underline{\chi}_k$

Step	Floating Pt. Operations	Data Storage (wds.)
1	17	16
2	7	34
3	19	55
4	268	36
5	97	36
6	3	3
Total	411	180

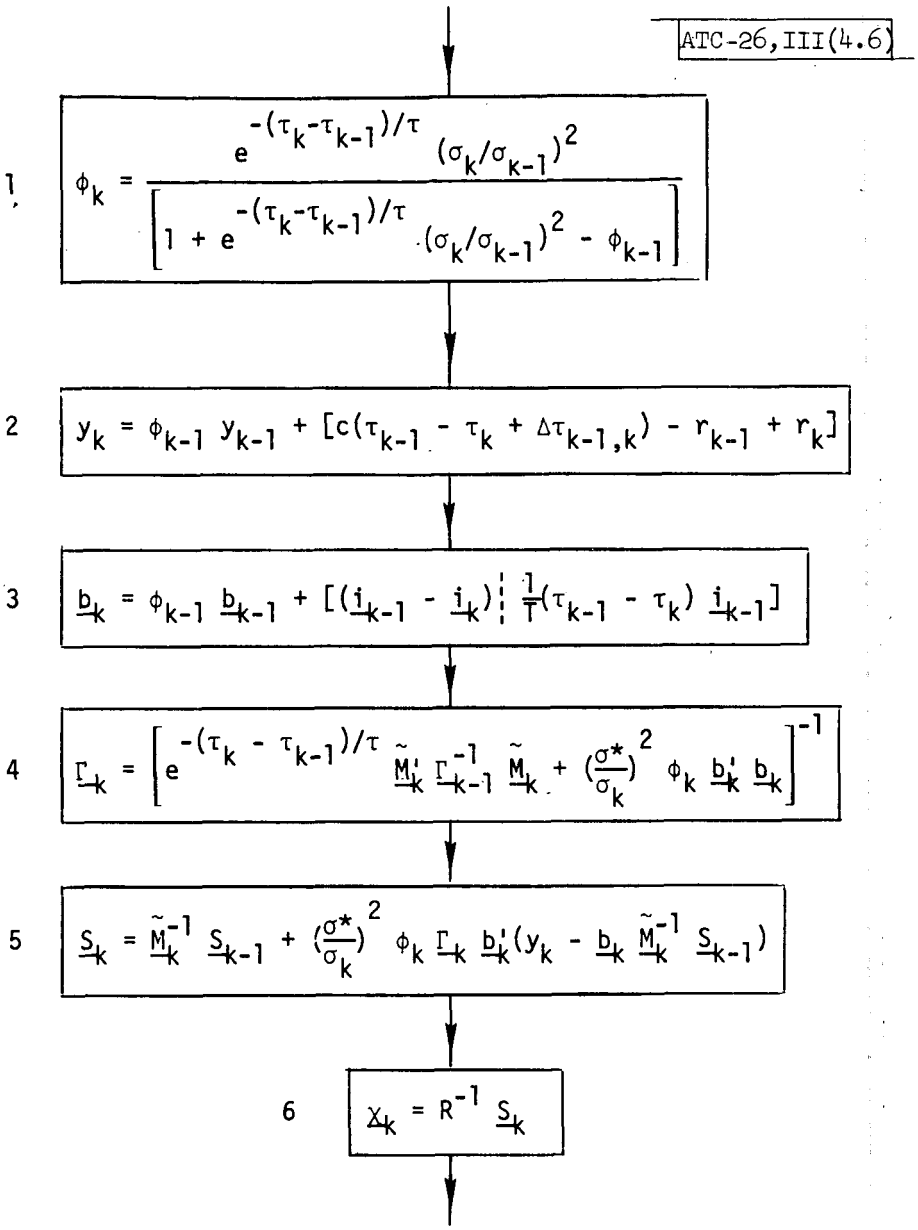

Fig. 4.6. Steps for updating $\underline{\chi}_k$.

SECTION V

AVIONICS

The avionics required to take advantage of the basic SAT navigation service consists of a top mounted antenna, an RF receiver, and an avionics computer. If air-derived position information is to be transmitted to the ground via the DABS data link, then a DABS transponder also is required.

The baseline system configuration has been chosen to facilitate the design of moderate-cost avionics. This section indicates how the antenna, receiver and avionics computer might be implemented.

5.1 RF AVIONICS

The block diagram of Fig. 5.1 depicts a suitable avionics package.

The antenna could be a top-mounted crossed-slot antenna with a nearly omnidirectional pattern over the upper hemisphere. Such a unit could be mass produced inexpensively using printed circuit dipoles and stripline techniques.

After heterodyning to 60 MHz, the signal is amplified and fed into the detector as indicated.

A block diagram of the detector is shown in Fig. 5.2. The detector performs three functions: 1) it estimates TOA using a synchronization demodulator; 2) it estimates TOA differences; and 3) it demodulates and decodes the data transmitted after the timing pulse. The indicated switch feeds the output of the IF amplifier to the synchronization demodulator until the timing pulse has been detected and its arrival time estimated.

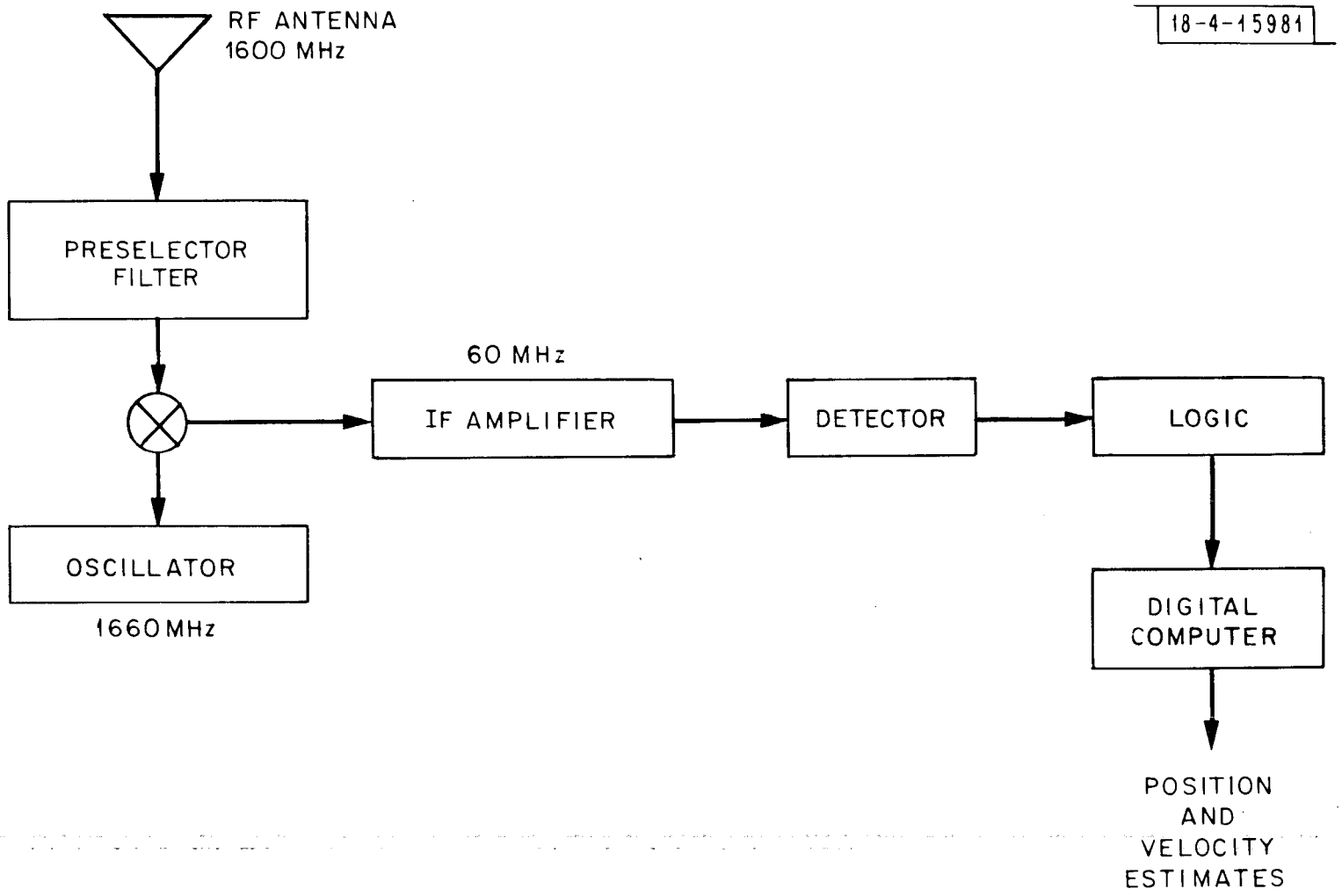

Fig. 5.1. Receiver avionics.

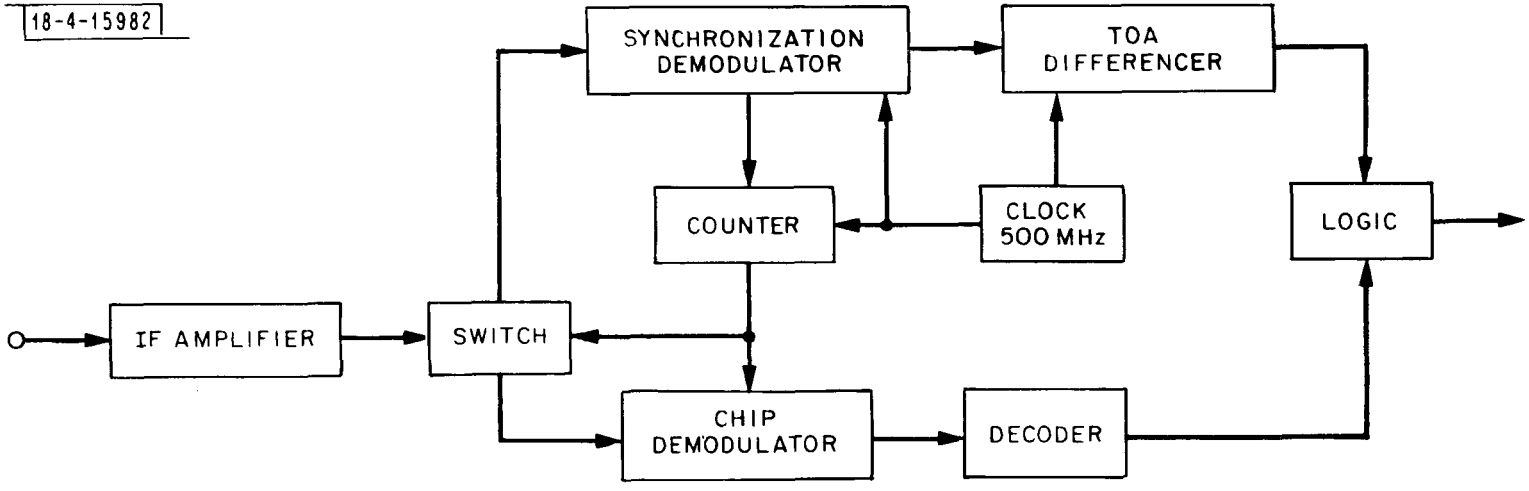

Fig. 5.2. Detector.

The counter is reset according to the estimated pulse arrival time. The counter activates the switch so that the data, beginning 1 msec after the timing pulse, enters the chip demodulator and decoder.

There are several ways to implement the synchronization and bit demodulators. As an example, an analog synchronization demodulator is diagrammed in Fig. 5.3. The dashed box is a block diagram of an analog DPSK bit demodulator. The output of the IF amplifier is passed through a filter matched to the chip shape (a 2 MHz bandpass filter would suffice for this design). The output of the matched filter is multiplied by a delayed version* of itself to determine the presence or absence of a polarity change. The multiplication effectively demodulates the IF signal to baseband, with the harmonics discarded by the low pass filter.

After emerging from the DPSK bit demodulator, the entire timing pulse is passed through the matched filter. When the output of the pulse matched filter exceeds a threshold, the timing pulse is detected. When a detection occurs, the peak output of the matched filter is used to estimate the pulse arrival time. The matched filter could be implemented with standard digital techniques or could be implemented by an acoustic surface wave device.

After TOA estimation, the detector switches to the data demodulator. The chip demodulator for the data is similar to the dashed box in Fig. 5.3 but a separate circuit is required because the chip duration is different. After decoding, the data is passed to digital logic for entry to the computer.

5.2 AVIONICS COMPUTER

Table 5.1 presents a conservative estimate of the computational requirements for the position update algorithm described in Section 4.4

*It would be necessary to provide temperature compensation if an inexpensive IF delay line were used for the chip delay. The delay line might be physically located in the same temperature controlled unit as the master crystal oscillator.

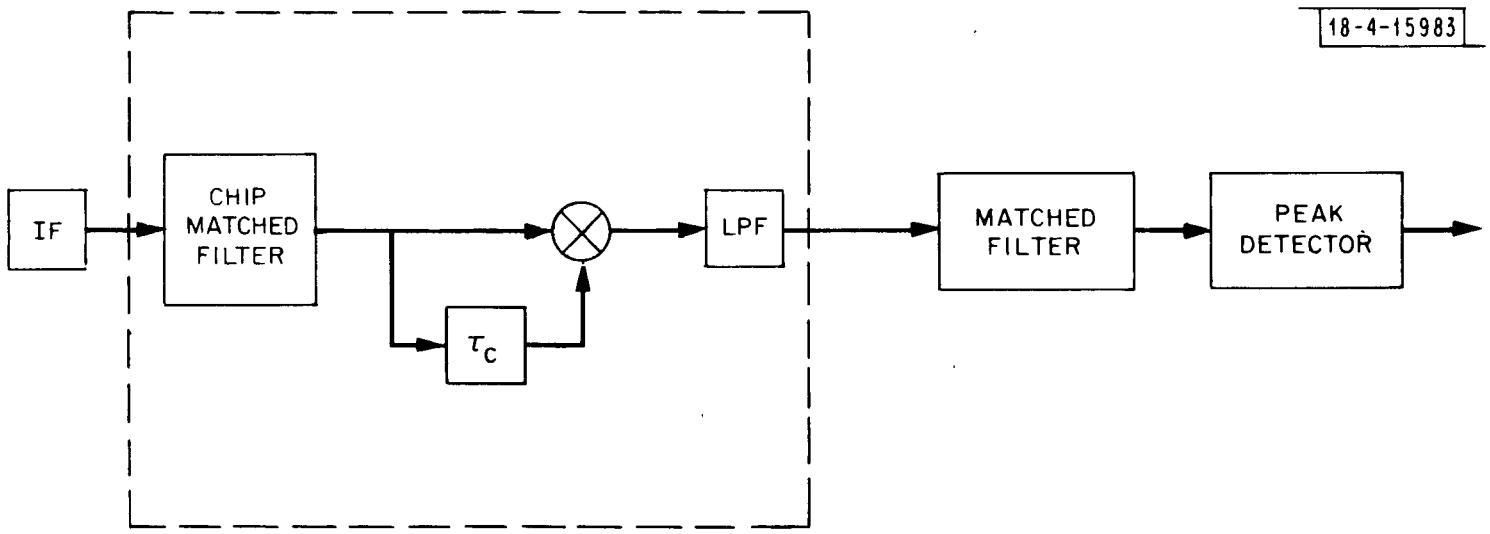

Fig. 5.3. Analog IF synchronization demodulator.

The computer's processor must execute approximately 11,000 floating point instructions per second. The bulk of the instructions are associated with the aircraft position determination calculation.

Approximately 360 words of random access memory (RAM) are required for data that changes with time. The RAM words must have at least 28 bits of fraction to ensure that round-off errors are negligible compared to the other sources of error. For purposes of the baseline design, it is assumed that RAM words consist of 32 bits of fraction, and 16 bits of exponent, or 48 bits total.

In addition to the RAM, approximately 3,100 words of read only memory (ROM) are required. The ROM contains trigonometric tables and frequently used constants as well as the program that drives the machine. Approximately 400 words are required for tables and constants. The program size can be estimated by using the (conservative) rule of thumb of five machine instructions per floating point operation. The program performs approximately 10,900/20 = 545 floating point operations following receipt of a TOA. Thus the program size is estimated at 2,700 ($\approx$5 x 545) words. Sixteen-bit words suffice in the portion of the ROM that contains the program. Forty-eight bit words are required in the remainder of the ROM.

With clever programming, it may be possible to avoid floating point operations. For purposes of the baseline system, however, it was assumed that the floating point operations are necessary. In addition to the floating point instructions, a representative set of jump, bit manipulation and I/O instructions are required.

While these computing requirements could be satisfied by a conventional sixteen bit mini-computer, this is not recommended because of undesirable cost and operational implications. The cost objections are as follows:

1. Use of a conventional machine involves placing the program and tables in (expensive) RAM as opposed to (inexpensive) ROM.
2. The T^2L logic used in conventional processors requires a power supply that contributes significantly to cost.

The operational problem is that the program and tables must be reloaded prior to each use.

It is more cost-effective and more practical to use special purpose digital hardware to satisfy the computing requirements of Table 5.1. A special purpose machine can be built entirely from off-the-shelf integrated circuits (ICs) or it can employ custom LSI chips* in addition to off-the-shelf ICs.

Figure 5.4 depicts a machine architecture that can be realized either way. The high-speed ROM shown contains a microprogram that realizes the basic instruction set.

Table 5.2 lists the requirements of the machine in terms of off-the-shelf integrated circuits. Table 5.3 indicates the estimated manufacturing costs of the machine. Note that the power supply required to drive the T^2L logic in the processor contributes significantly to the total cost.

Presumably the cost of the machine could be reduced by putting all or part of the processor into custom integrated circuit chips. For example,

*For example the Hewlett-Packard pocket calculator employs five custom LSI chips.

putting the entire processor into custom NMOS chips would not only reduce parts and assembly costs but would also obviate the need for an expensive power supply.

TABLE 5.1

ESTIMATED COMPUTATIONAL REQUIREMENTS
(10 Satellites in View)

	Floating Pt. Operations Per Sec	Random Access Memory	Read Only Memory
Satellite Position	400	90	0
Aircraft Position	10,000	250	30
Coordinate Trans.	500	20	370
Program	0	0	2,700
Total	10,900	360	3,100

TABLE 5.2

ESTIMATED IC REQUIREMENTS

	IC Packages	Technology	Parts & Assembly Cost (in dollars)
Processor			
Arith. Unit	40	T^2L	100
Controller	100	T^2L	250
H.S. ROM	8	T^2L	80
Power Supply			150
L.S. ROM	4	MOS	100
RAM	16	MOS	150
Misc. CKT	20	T^2L	50
Total	188		880

TABLE 5.3

ESTIMATED MANUFACTURING COST

Parts & Assembly	$ 880
PC boards (2)	$ 50
Test	$ 150
Total	$1,080

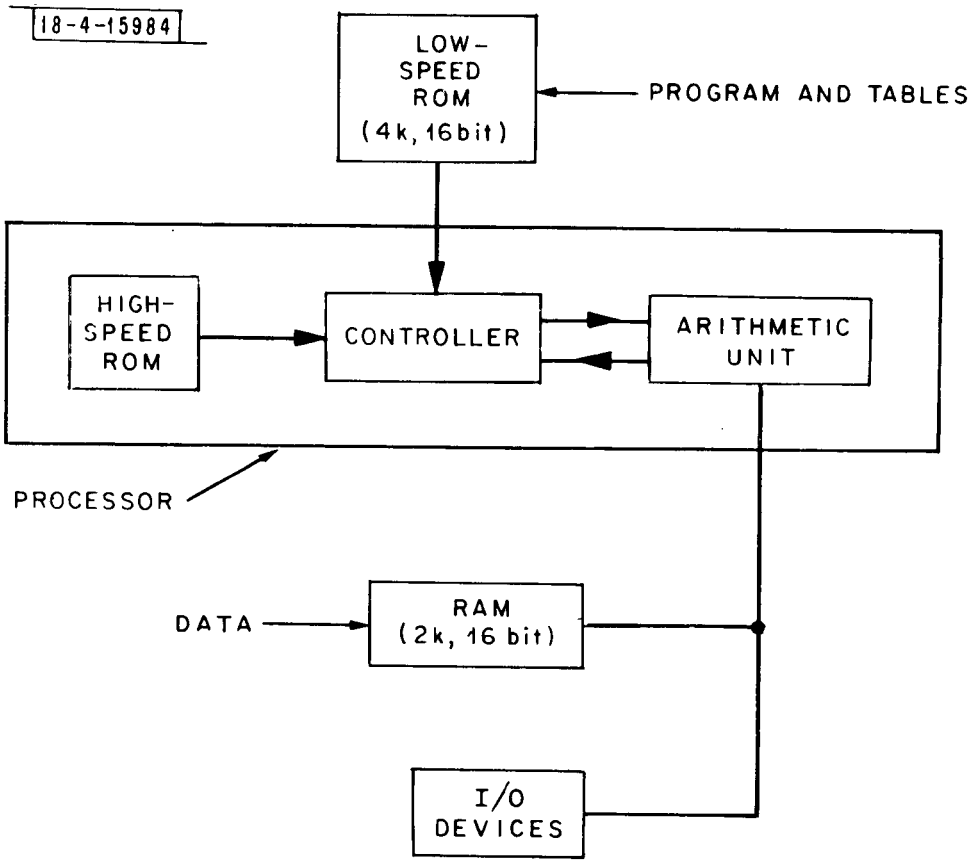

Fig. 5.4. Computer block diagram.

SECTION VI

AIR-TO-GROUND LINK

The air-derived position information could be transmitted to the ground for inclusion in the ATC data base as diagrammed in Fig. 1.1. The information could be used to extend surveillance coverage to airports without towers. The information could also be used to provide surveillance services to en route aircraft beyond normal coverage.

It should be noted that use of air-derived position information for surveillance purposes makes surveillance dependent upon aircraft equipment. Nonetheless, use of such information may represent a cost-effective method of extending surveillance coverage.

The air-to-ground link can be implemented in several ways. The baseline system utilizes the DABS data link. An alternative implementation consists of a communications satellite. This section discusses both approaches.

6.1 THE DABS IMPLEMENTATION

For the purposes of the baseline system it is assumed that the air-derived position information is transmitted to the ground via the DABS down-link.

In areas already serviced by DABS, the air-derived position estimates would provide a backup to the normal ground-derived position data. Near the maximum range of a DAB interrogator/receiver, the air-derived position estimates might actually be more accurate than the ground-derived (range-azimuth) position estimates.

In areas not serviced by DABS, extended coverage could be obtained by utilizing an "austere" DABS ground installation. Each austere DABS installation would interrogate aircraft in its vicinity and telemeter the position (as determined by the SAT on-board processor) to the nearest FAA center.

Table 6.1 gives the number of bits required to send the position of the aircraft in increments of 100 ft allowing coverage throughout CONUS with a maximum reportable altitude of 50,000 ft. This information could be sent without altering the DABS transponder.

It is reasonable to anticipate a savings in cost for an austere DABS installation compared to a conventional DABS installation. For example, the austere DABS antenna could consist of a fixed (non-rotating) vertical dipole array having an omnidirectional pattern in azimuth and a sharp vertical cut-off at the horizon. In addition to being less expensive to manufacture than a directional antenna, the austere antenna would require no moving mount and no electronic switching; it could be installed easily on a modest tower. Furthermore, the austere DABS receiver would not require a capability to accurately measure range or azimuth. Finally a small local computer should suffice for the austere DABS installation since such facilities would provide surveillance service only for low-density airspace and could be controlled from a neighboring full DABS installation.

The downlink determines the effective range of an austere DABS interrogator/receiver. Table 6.2 presents a representative downlink power budget for an aircraft at a range of 45 miles and an elevation angle $\varepsilon = 1°$. It is assumed

TABLE 6.1

BIT REQUIREMENTS FOR POSITION REPORTING
(100 FT INCREMENTS)

Altitude	9 bits
Longitude	14 bits
Latitude	14 bits
Identity	20 bits
Error detection	3 bits
Total	60 bits

that the effective radiated power (ERP) from the aircraft is at least 100 w.* The austere DABS antenna is assumed to have 4 dB gain at $\varepsilon = 1°$, with a 4 dB/degree roll off in the region $|\varepsilon| < 1.5°$. The 4.5 dB multipath fading loss accounts for (worst case) specular reflection from a flat earth with a unity reflection coefficient. Since the antenna is omnidirectional in azimuth, only the first 200 nsec of the received pulse is used to provide some protection against multipath reflections from vertical objects such as buildings and mountains. An additional 6 dB loss is assumed to account for frequency offset, time synchronization errors and other implementation errors. The effective receiver noise temperature of 1,000°K is readily achievable with today's moderate cost RF front ends. The probability of bit error implied by the 14.5 dB signal-to-noise ratio (E/N_0) depends on the modulation. For example, for incoherent PAM with an appropriate choice of threshold, the value E/N_0 = 14.5 dB can result in a 10^{-3} bit error probability.†

The region of airspace corresponding to an E/N_0 of at least 14.5 dB is shown in Fig. 6.1. The figure includes the effects of both earth curvature and atmospheric refraction.‡ The shaded area also accounts for reflection multipath fading loss, for the assumed antenna characteristics. The lower curve indicates the coverage that could be obtained with "down-to-the horizon visibility," and no E/N_0 constraint. The middle curve indicates the boundary of possible values for visibility down to an elevation angle of 0.5° with no E/N_0 constraint.

*ERP equals the product of the radiated power and the aircraft antenna gain in the direction of the DABS ground site.

†Use $P_{e,b} < e^{-E/4N_o}$. See 13.

‡The "4/3 earth model" was used for this purpose. See 14,15.

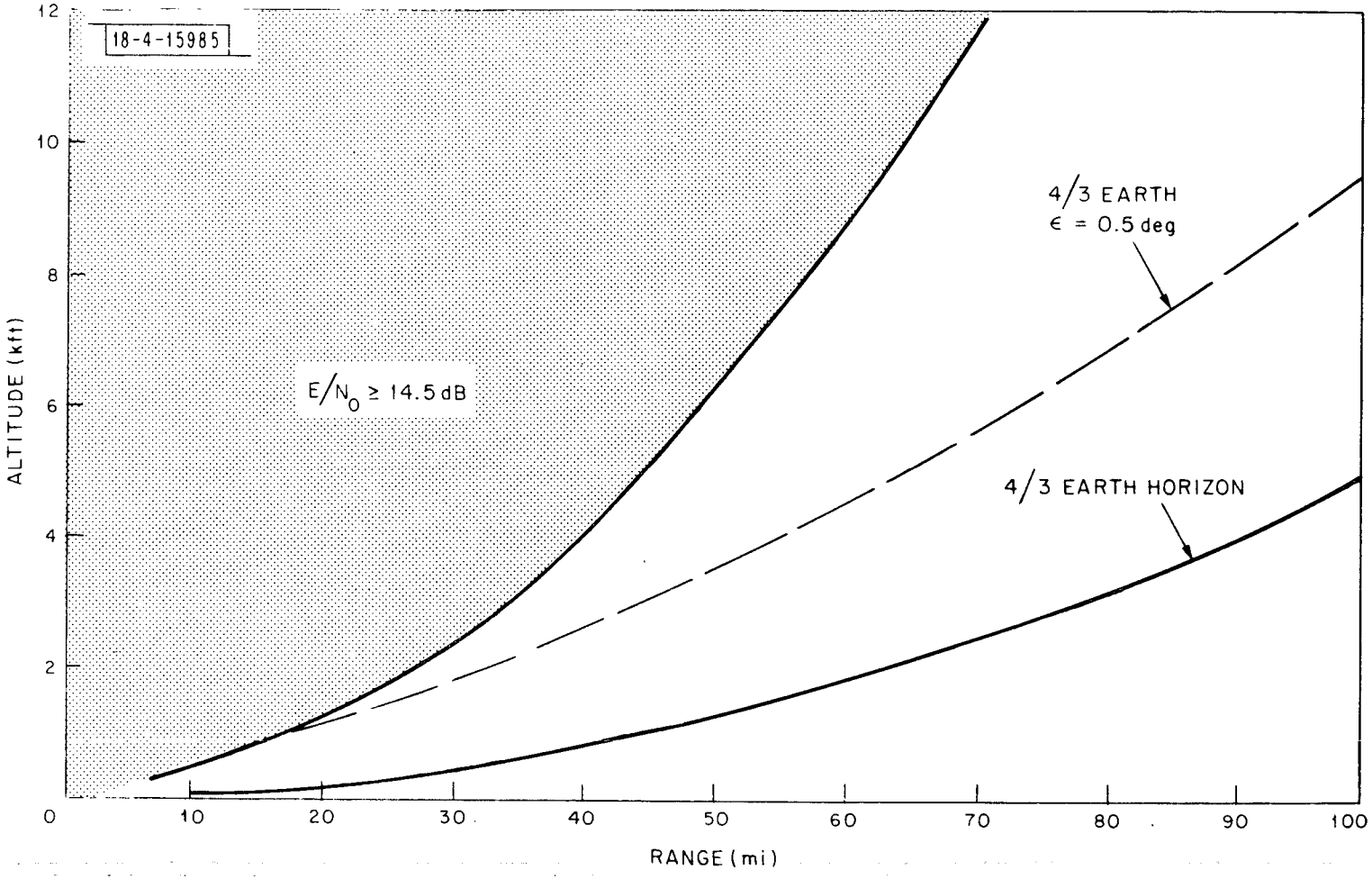

Fig. 6.1. Graph showing coverage.

TABLE 6.2

AIR-TO-GROUND POWER BUDGET

Aircraft ERP	-20 dBW	Minimum radiated power
Path Loss	-131 dB	45 miles at 1090 MHz
Antenna Gain	4 dB	At 1° elevation angle
Multipath Fading Loss	-4.5 dB	Antenna pattern slope 4 dB/degree
Pulse Duration	-67 dB sec	200 nsec
Mismatched Filter Loss	-6 dB	Frequency drift, synchronization error, manufacturing tolerance
Noise Power Density	-199 dBW/Hz	1000°K equivalent noise temperature
Received Signal-to-Noise Ratio	14.5 dB	E/N_o

If the air-to-ground link were realized by the DABS data link, the baseline system could straightforwardly be integrated into the Upgraded Third Generation System. Specifically, air-derived position information could be incorporated into the data base in a manner similar to other DABS-derived position information.

6.2 COMMUNICATIONS SATELLITE IMPLEMENTATION

An alternative implementation of the air-to-ground link could employ a communications satellite. The primary advantage of this realization is its "down to the ground" coverage.

Any one of the following methods could be used to transmit position information to the satellite(s).

1. The aircraft could report at random intervals.
2. Aircraft transmissions could be coordinated by adding to the epoch time (transmitted from the satellites) a delay based on aircraft identity and aircraft position.
3. The aircraft could respond to satellite interrogation.

Methods 1 and 2 introduce some garbling (multiple access noise) due to simultaneous reception of messages from several aircraft. Method 3 introduces a substantial centralized scheduling problem.

A first order analysis of Method 1 is given in Appendix D. It is concluded that for reasonable system parameters, a relay satellite could support in excess of 38,000 aircraft at an update rate of once every 10 sec with a probability of message error smaller than one tenth.

The peak instantaneous airborne count may exceed 38,000 aircraft during the 1990-2000 time frame, but a majority of the aircraft would be under DABS surveillance. Thus using DABS all-call lockout to prevent aircraft from reporting via satellite when they are under DABS control, a satellite link should have sufficient capacity to maintain cooperative surveillance on all CONUS aircraft not covered by DABS.

In spite of the fact that adequate extended surveillance coverage could be achieved by means of a satellite link, several other factors argue against use of such a link. Whereas the "austere DABS" realization uses DABS avionics for communication service, additional expensive avionics (including a transmitter) is required for the satellite communication link. In addition, the ground-based realization is relatively insensitive to jamming due to its distributed nature. By contrast, the satellite implementation is highly vulnerable to jamming. Finally with a ground based implementation, gradual deployment to selected airspace is possible. In the case of the satellite implementation, however, a large initial commitment must be made with the launch of the communication satellite repeaters.

REFERENCES

1. B.D. Elrod and J.J. Fee, "Preliminary Analysis of the ASTRO-NAV Concept," MITRE Corp. Report MTR-6478, McLean, Virginia (October 1973).

2. "Final Report - Advanced Air Traffic Management System," Rockwell International Corporation, Autonetics Division, Report No. C72-1206/201; Anaheim, California (April 1973).

3. L. Schuchman, "The ASTRO-DABS Concept," MITRE Corp. Technical Report MTR-6287, McLean, Virginia (November 1972).

4. "Advanced Air Traffic Management - System B Summary Report," MITRE Corp. Report MTR-6419, McLean, Virginia (May 1973).

5. "Study and Concept Formulation of a Fourth Generation Air Traffic Control System," I-V, Boeing Company, Report DOT-TSC-3601-1, Renton, Wash., D.C. (April 1972).

6. P.M. Diamond, "The Potential of a System of Satellites as a Part of an Air Traffic Control System," AGARD Conference Proceedings No. 105, 20-1, (June 1972).

7. D.D. Otten, "Study of a Navigation and Traffic Control Technique Employing Satellites," I-IV, TRW Systems Group Report No. 08710-6012-12000, Redondo Beach, California (December 1967).

8. K.D. McDonald, "A Survey of Satellite-Based Systems for Navigation Position Surveillance, Traffic Control and Collision Avoidance," Addendum to Proceedings of ION National Airspace Meeting, The Inst. of Nav., Wash., D.C. (March 1973).

9. K.S. Schneider, I.G. Stiglitz, and A.E. Eckberg, "Surveillance Aspects of the Advanced Air Traffic Management System," Lincoln Laboratory, M.I.T. Project Report ATC-10 (22 June 1972).

10. R.S. Orr and K.S. Schneider, "Technical Assessment of Satellites for CONUS Air Traffic Control. Vol. I: Coordinated Aircraft-to-Satellite Techniques," Project Report ATC-26, Lincoln Laboratory, M.I.T. (to be published).

11. K.S. Schneider and R.S. Orr, "Technical Assessment of Satellites for CONUS Air Traffic Control. Vol. II: Random Access Aircraft-to-Satellite Techniques," Project Report ATC-26, Lincoln Laboratory, M.I.T. (to be published).

12. I.G. Stiglitz, et.al. "Concept Formulation Studies of the Surveillance Aspects of the Fourth Generation Air Traffic Control System," Lincoln Laboratory, M.I.T. Project Report ATC-7, 187 (21 September 1971).

13. E. Arthurs and H. Dym, "On the Optimum Detection of Digital Signals in the Presence of White Gaussian Noise - A Geometric Interpretation and a Study of Three Basic Data Transmission Systems," IRE Trans. Comm. Systems, 336-372 (December 1962).

14. B.R. Bean and G.D. Thayer, "Models of the Atmospheric Radio Refractive Index," Proc. IRE, 740-756 (May 1959).

15. W.T. Fishback, "Methods for Calculating Field Strength with Standard Refraction," 115 in D.E. Kerr, Propagation of Short Radio Waves, McGraw-Hill Book Co. (1951).

16. H.L. Van Trees, Detection, Estimation and Modulation Theory, I, John Wiley and Sons, New York (1968).

17. J.M. Wozencraft and I.M. Jacobs, Principles of Communication Engineering, John Wiley and Sons, New York (1965).

18. R.S. Orr and R.D. Yates, "On the Estimation of the Arrival Time of Pulse Signals in Gaussian Noise," Lincoln Laboratory, M.I.T. Technical Note to be published.

19. D.A. Shnidman, "A Comparison of Immunity to Garbling for Three Candidate Modulation Schemes for DABS," Lincoln Laboratory, M.I.T. Project Report ATC-12, (14 August 1972).

APPENDIX A

ERRORS DUE TO NOISE

The 22 dB signal-to-noise ratio for the timing pulse ensures that a detection threshold can be selected to produce a high probability of detection (P_d) and a low probability of false alarm (P_f). Specifically, for ideal Gaussian noise P_d and P_f are related as follows:

$$P_d = Q\left(\sqrt{\frac{2E}{N_o}}\ ,\ \sqrt{-2\ln P_f}\right) \tag{A.1}$$

where Q denotes the Marcum Q function.* Thus for example, for $P_f = 5 \times 10^{-15}$, the corresponding detection probability is

$$\begin{aligned} P_d &= Q(\alpha,B)\Big|_{\substack{\alpha = \sqrt{2E/N_o} = 17.8 \\ \beta = \sqrt{-2\ln P_f} = 8.12}} \\ &\approx 1 - \frac{1}{(\alpha-B)}\left(\frac{\beta}{2\pi\alpha}\right)^{1/2} e^{-(\alpha-B)^2/2} \\ &= 1 - 1.25 \times 10^{-22} \end{aligned} \tag{A.2}$$

Presumably the noise is confined by filtering to the 2 MHz frequency band occupied by the timing pulse. Thus the false alarm rate can be estimated as follows

*See Ref. 16, pages 344-345, 395.

$$\text{False Alarm Rate} \approx (2\ \text{MHz})\ (P_f)$$

$$= 10^{-8}/\text{sec}$$

$$= 8.4 \times 10^{-4}/\text{day} \qquad \text{(A.3)}$$

The signal to noise ratio for data chips is as follows

$$\frac{E_c}{N_o} = 12\ \text{dB} \qquad \text{(A.4)}$$

For DPSK the bit error probability* is given by

$$P_e = \frac{1}{2}\ e^{-E_c/N_o} = 6.5 \times 10^{-8} \qquad \text{(A.5)}$$

*Ref. 17, page 525.

APPENDIX B

POLYNOMIAL APPROXIMATION OF SATELLITE TRAJECTORY

This appendix describes a simple procedure for extrapolating satellite position. The procedure uses (ground predicted) position and velocity information for time τ_1 to predict satellite position before and after τ_1. Given exact position and velocity information for time τ_1, the procedure predicts satellite position to better than one foot over the one hundred second interval $(\tau_1 - 50) \leq \tau \leq (\tau_1 + 50)$.

The procedure consists of a third order Taylor series approximation to the satellite trajectory. While a Tschebyscheff or least squares approximation may produce a better result, the Taylor series development considered here shows that polynomial approximations exist that are both simple and accurate.

The appendix is divided into four sections as follows.

1. Review of the Exact Satellite Trajectory
2. Taylor Series Approximation of the Trajectory
3. Bound on the Error
4. Proof of a Necessary Inequality

Step 1: Review of the Exact Satellite Trajectory

The motion of any body near the earth is governed by Newton's law:

$$\underline{r}''(\tau) = - \gamma M \frac{1}{|\underline{r}(\tau)|^3} \underline{r}(\tau) \qquad (B.1)$$

where

$\underline{r}(\tau)$ = A (3x1) vector specifying the body's position relative to the earth's center.

γ = The universal gravitational constant

M = The mass of the earth

For the (low) initial velocities characteristic of satellites, the solution $\underline{r}(\tau)$ of (B.1) traces out an ellipse, having the earth as a focus. Newton's Law (B.1) can be rewritten in terms of parameters of the elliptical orbit as follows

$$\underline{r}''(\tau) = -\left(\frac{2\pi}{T}\right)^2 \frac{R^3}{|\underline{r}(\tau)|^3}\, \underline{r}(\tau) \qquad (B.2)$$

where

T = The orbital period

R = The length of the semi-major axis of the ellipse.

For a synchronous orbit T = 1 day = 86,400 seconds and R $\approx$ 26,000 miles.

If one defines the x axis of an earth centered coordinate system to coincide with the major axis of the ellipse and the z axis to be perpendicular to the plane of the ellipse, then the detailed solution of (B.1) is

$$\underline{r}(\tau) = \begin{bmatrix} r_x(\tau) \\ r_y(\tau) \\ r_z(\tau) \end{bmatrix} = R \begin{bmatrix} \cos\phi(\tau) - e \\ \sqrt{1 - e^2}\,\sin\phi(\tau) \\ 0 \end{bmatrix} \qquad (B.3)$$

The quantity e in (B.3) is the eccentricity of the orbit (between 0 and 0.4 for most synchronous satellites), and $\phi(\tau)$ is the eccentric anomaly which satisfies the following equation

$$\phi(\tau) - e \sin \phi(\tau) = \frac{2\pi}{T} (\tau - \tau_p) \tag{B.4}$$

(τ_p is the time of passage through the perigee).

Step 2: Taylor Series Approximation of the Trajectory

A family of simple polynomial approximations to the actual trajectory can be developed by expanding (B.3) into a Taylor series about a reference time τ_1. Specifically Taylor's theorem asserts that

$$\underline{r}(\tau) = \underline{r}(\tau_1) + \frac{(\tau - \tau_1)}{1!} \underline{r}'(\tau_1) + \frac{(\tau - \tau_1)^2}{2!} \underline{r}''(\tau_1) \ldots + \frac{(\tau - \tau_1)^{N-1}}{(n-1)!} \underline{r}^{(N-1)}(\tau_1) + \frac{(\tau - \tau_1)^n}{n!} \underline{r}^{(n)}(s) \tag{B.5}$$

where the argument s in the remainder term denotes some value of time between τ_1 and τ. The derivative $\underline{r}'(\tau_1)$ corresponds to the satellite velocity $\underline{v}(\tau_1)$ at time τ_1. The higher order derivatives can be evaluated using (B.2) and the following relationships derived from (B.3) and (B.4)

$$|\underline{r}(\tau_1)| = \left([r_x(\tau_1)]^2 + [r_y(\tau_1)]^2 \right)^{1/2}$$

$$= R[1 - e \cos \phi(\tau_1)] \tag{B.6}$$

$$\phi'(\tau_1) = \frac{2\pi}{T} \frac{1}{1 - e \cos \phi(\tau_1)}$$

$$= \frac{2\pi}{T} \frac{R}{|\underline{r}(\tau_1)|} \tag{B.7}$$

The third order Taylor approximation is considered here. Differentiation of (B.2) indicates that

$$\underline{r}'''(\tau_1) = \omega_o^2 \left[-\frac{3}{|\underline{r}(\tau)|} \frac{d|\underline{r}|}{d\tau} \underline{r}(\tau) + \frac{d\underline{r}}{d\tau} \right]_{\tau=\tau_1}$$

$$= \omega_o^2 \left[-\frac{3\{\underline{v}(\tau_1) \cdot \underline{r}(\tau_1)\}}{|\underline{r}(\tau_1)|^2} \underline{r}(\tau_1) + \underline{v}(\tau_1) \right] \tag{B.8}$$

where

$$\omega_o^2 \triangleq \left(\frac{2\pi}{T}\right)^2 \frac{R^3}{|\underline{r}(\tau_1)|^3} \tag{B.9}$$

Thus the third order Taylor approximation takes the form

$$\hat{\underline{r}}(\tau) = \underline{r}(\tau_1) + (\tau - \tau_1)\,\underline{r}'(\tau_1) + \frac{(t - \tau_1)^2}{2!}\,\underline{r}''(\tau_1) + \frac{(\tau - \tau_1)^3}{3!}\,\underline{r}'''(\tau_1)$$

$$= \left[1 - \frac{\omega_o^2}{2}(\tau - \tau_1)^2 - \frac{\omega_o^2}{2}\left(\frac{\underline{v}(\tau_1) \cdot \underline{r}(\tau_1)}{\underline{r}(\tau_1) \cdot \underline{r}(\tau_1)}\right)(\tau - \tau_1)^3 \right] \underline{r}(\tau_1)$$

$$+ \left[(\tau - \tau_1) + \frac{\omega_o^2}{6}(\tau - \tau_1)^3 \right] \underline{v}(\tau_1) \tag{B.10}$$

Step 3: Bound on the Error

The approximation (B.10) makes the error

$$\hat{\underline{r}}(\tau) - \underline{r}(\tau) = -\frac{(\tau - \tau_1)^4}{4!}\,\underline{r}''''(s) \tag{B.11}$$

It is shown subsequently that $\underline{r}''''(s)$ is bounded as follows for $e \leq 0.4$

$$|\underline{r}''''(s)| \leq 140\,(\tfrac{2\pi}{T})^4\,R \tag{B.12}$$

Use of (B.12) in (B.11) indicates

$$\left|\hat{\underline{r}}(\tau) - \underline{r}(\tau)\right| \leq 5.83\left[\frac{2\pi(\tau - \tau_1)}{T}\right]^4 R \tag{B.13}$$

Thus for $|\tau - \tau_1| \leq 50$, T = 1 day = 84,000 sec and R = 26,000 miles

$$|\hat{\underline{r}}(\tau) - \underline{r}(\tau)| \leq 0.16 \text{ ft} \tag{B.14}$$

Step 4: Proof of (B.12)

Straightforward differentiation of (B.3) and (B.6), together with use of (B.7) shows that the first and second derivatives of $\underline{r}$ and $|\underline{r}|$ satisfy the following relationships

$$\left|\frac{d\underline{r}}{d\tau}\right| \leq \frac{2\pi}{T}\,\frac{R^2}{|\underline{r}|} \tag{B.15}$$

$$\left|\frac{d|\underline{r}|}{d\tau}\right| \leq e\left|\frac{d\underline{r}}{d\tau}\right| \leq e\,\frac{2\pi}{T}\,\frac{R^2}{|\underline{r}|} \tag{B.16}$$

$$\left|\frac{d^2\underline{r}}{d\tau^2}\right| = \left(\frac{2\pi}{T}\right)^2 \frac{R^3}{|\underline{r}|^2} \tag{B.17}$$

$$\left|\frac{d^2|\underline{r}|}{d\tau^2}\right| \leq e\left|\frac{d^2\underline{r}}{d\tau^2}\right| = e\left(\frac{2\pi}{T}\right)^2 \frac{R^3}{|\underline{r}|^2} \tag{B.18}$$

Differentiation of (B.2) gives

$$\frac{d^4\underline{r}}{d\tau^4} = -\left(\frac{2\pi}{T}\right)^2 R^3 \left[\frac{12}{|\underline{r}|^5}\left(\frac{d|\underline{r}|}{d\tau}\right)^2 \underline{r} - \frac{3}{|\underline{r}|^4}\,\frac{d^2|\underline{r}|}{d\tau^2}\,\underline{r} - \frac{6}{|\underline{r}|^4}\,\frac{d|\underline{r}|}{d\tau}\,\frac{d\underline{r}}{d\tau} + \frac{1}{|\underline{r}|^3}\,\frac{d^2\underline{r}}{d\tau^2}\right] \tag{B.19}$$

It follows that

$$\left|\frac{d^4\underline{r}}{d\tau^4}\right| \leq \left(\frac{2\pi}{T}\right)^2 R^3 \left[\frac{12}{|\underline{r}|^4}\left(\frac{d|\underline{r}|}{d\tau}\right)^2 + \frac{3}{|\underline{r}|^3}\,\frac{d^2|\underline{r}|}{d\tau^2} + \frac{6}{|\underline{r}|^4}\left|\frac{d|\underline{r}|}{d\tau}\right|\left|\frac{d\underline{r}}{dt}\right| + \frac{1}{|\underline{r}|^3}\left|\frac{d^2\underline{r}}{d\tau^2}\right|\right] \tag{B.20}$$

Use of (B.15)-(B.18) in (B.20) gives

$$\left|\frac{d^4\underline{r}}{d\tau^4}\right| \leq \left(\frac{2\pi}{T}\right)^4 R \left[(12\ e^2 + 6e)\left(\frac{R}{|\underline{r}|}\right)^6 + (3e + 1)\left(\frac{R}{|\underline{r}|}\right)^5\right]$$

$$\leq \left(\frac{2\pi}{T}\right)^4 R \frac{1}{(1-e)^6}\ \left[12\ e^2 + 9e + 1\right] \qquad \text{(B.21)}$$

Thus for $e \leq 0.4$,

$$\left|\frac{d^4\underline{r}}{d\tau^4}\right| \leq 140\ \left(\frac{2\pi}{T}\right)^4 R \qquad \text{(B.22)}$$

APPENDIX C

DERIVATIONS FOR SECTION 4

C.1 LEAST SQUARES SOLUTION OF EQUATIONS (4.3.1)

The least squares solution of (4.3.1) minimizes the error measure

$$E_k = \underline{\varepsilon}_k' \, \underline{P}_k^{-1} \, \underline{\varepsilon}_k \qquad \text{(C.1.1)}$$

$$= \frac{1}{c^2} \left[\underline{K}_k - (cT_0)\, \underline{1}_k - \underline{F}_k \, \underline{X}\right]' \, \underline{P}_k^{-1} \left[\underline{K}_k - (cT_0)\, \underline{1}_k - \underline{F}_k \, \underline{X}\right]$$

The minimizing condition $\partial E_k / \partial T_0 = 0$ requires

$$\underline{1}_k' \, \underline{P}_k^{-1} \left[\underline{K}_k - (cT_0)\, \underline{1}_k - \underline{F}_k \, \underline{X}\right] = 0 \qquad \text{(C.1.2)}$$

or equivalently

$$(cT_0) = \frac{1}{(\underline{1}_k' \, \underline{P}_k^{-1} \, \underline{1}_k)} \, \underline{1}_k' \, \underline{P}_k^{-1} \left[\underline{K}_k - \underline{F}_k \, \underline{X}\right] \qquad \text{(C.1.3)}$$

Use of (C.1.3) to eliminate (cT_0) from (C.1.2) leads to the modified error measure

$$E'_k = E_k \Big| \, \partial E / \partial T_0 = 0$$

$$= \frac{1}{c^2} \left[\underline{K}_k - \underline{F}_k \, \underline{X}\right]' \, \underline{Q}_k \left[\underline{K}_k - \underline{F}_k \, \underline{X}\right] \qquad \text{(C.1.4)}$$

where

$$\underline{Q}_k = \underline{P}_k^{-1} - \frac{1}{(\underline{1}_k' \underline{P}_k^{-1} \underline{1})} \underline{P}_k^{-1} \underline{1}_k \underline{1}_k' \underline{P}_k^{-1} \qquad (C.1.5)$$

The additional minimizing conditions $\partial E_k'/\partial \underline{x} = 0$ require

$$\underline{F}_k' \underline{Q}_k [\underline{K}_k - F_k \underline{X}] = 0 \qquad (C.1.6)$$

Solution of (C.1.6) for $\underline{X}$ yields

$$\hat{\underline{X}} = [\underline{F}_k' \underline{Q}_k \underline{F}_k]^{-1} \underline{F}_k' \underline{Q}_k \underline{K}_k \qquad (C.1.7)$$

C.2 MOTIONAL ERROR

This appendix examines the motional error (4.3.13). The examination is carried out in the following steps.

1. The effect on the error (4.4.13) of changing the signaling sequence is clarified.
2. The mean of the motional error over all signaling sequences is evaluated.
3. The covariance matrix is calculated for the deviation of the motional error from its mean.
4. The results are specialized to the satellite constellation of Figure 4.3, assuming the aircraft flies in the α direction with constant velocity $\underline{V}_\alpha$.

Step 1: Effect on (4.3.13) of a Change in Signaling Sequence

Changing the signaling sequence amounts to

1. Permuting the rows of $\underline{F}_k$
2. Permuting the rows and columns of $\underline{Q}_k$

These operations correspond respectively to the substitutions

$$\underline{F}_k \rightarrow \underline{C}\,\underline{F}_k$$

$$\underline{Q}_k \rightarrow \underline{C}\,\underline{Q}_k\,\underline{C}'$$

where $\underline{C}$ is a k x k "permutation matrix". Thus the expression (4.3.13) for the motional error takes the following form for any new signaling sequence.

$$\hat{\underline{X}}_{\tau k} - \underline{X}_{\tau k} = -\Delta T\,[\underline{F}_k'\,\underline{C}'\,\underline{C}\,\underline{Q}_k\,\underline{C}'\underline{C}\,\underline{F}_k]^{-1}\,\underline{F}'\,\underline{C}'\,\underline{C}\,\underline{Q}\,\underline{C}'\,\underline{S}_k\underline{C}\,\underline{F}\,\dot{\underline{X}} \qquad (C.2.1)$$

But

$$\underline{C}'\,\underline{C} = \underline{I} \qquad (C.2.2)$$

for any permutation matrix. Thus (C.2.1) reduces to

$$\hat{\underline{X}}_{\tau k} - \underline{X}_{\tau k} = -\Delta T\,[\underline{F}_k'\,\underline{Q}_k\,\underline{F}_k]^{-1}\,\underline{F}_k'\,\underline{Q}_k\,(\underline{C}'\underline{S}_k\,\underline{C})\,\underline{F}_k\,\dot{\underline{X}} \qquad (C.2.3)$$

Comparison of (4.3.13) with (C.2.3) shows that the expressions are identical except for the substitution

$$\underline{S}_k \rightarrow \underline{C}'\underline{S}_k\underline{C} \qquad (C.2.4)$$

Consequently changing the signaling sequence can be accounted for simply by correspondingly permuting the diagonal elements of the matrix $\underline{S}_k$ in (4.3.13).

Step 2: Evaluating the Mean of (4.3.13)

Changing the signaling sequence through all permutations amounts to permuting the diagonal elements of $\underline{S}_k$ in (4.3.13) in all possible ways. Thus for the purpose of computing first and second moments of (4.3.13) over all signaling sequences, the diagonal elements of $\underline{S}_k$ can be replaced by random variables $S_1, S_2, \ldots S_k$ having the following properties.

$$\overline{S_i} = \frac{[1 + 2\cdots+(k-1)]\,(k-1)!}{k!} = \frac{k-1}{2} \qquad (C.2.5)$$

$$\overline{(S_i)^2} = \frac{[1^2 + 2^2\cdots+(k-1)^2](k-1)!}{k!}$$

$$= \frac{(k-1)(2k-1)}{6} \qquad (C.2.6)$$

$$\overline{(S_i S_j)}_{i\neq j} = \frac{([1 + 2\cdots+(k-1)]^2 - [1^2 + 2^2\cdots+(k-1)^2])(k-2)!}{k!}$$

$$= \frac{k}{k-1}(\overline{S_i})^2 - \frac{1}{k-1}\overline{(S_i)^2} \qquad (C.2.7)$$

$$\overline{(S_i-\bar{S}_i)^2} = \overline{(S_i)^2} - (\bar{S}_i)^2$$

$$= \frac{k(k+1)}{12} - \frac{k+1}{12} \qquad \text{(C .2.8)}$$

$$\overline{(S_i-\bar{S}_i)(S_j-\bar{S}_j)} = \overline{(S_iS_j)} - (\bar{S}_i)(\bar{S}_j)$$

$$i\neq j \qquad = -\frac{k+1}{12} \qquad \text{(C .2.9)}$$

That is, Eq. (4.3.13) can be rewritten

$$\hat{\underline{X}}_{\tau k} - \underline{X}_{\tau k} = -\Delta T\,[\underline{F}_k'\,\underline{Q}_k\,\underline{F}_k]^{-1}\;\underline{F}_k'\,\underline{Q}_k\,\tilde{\underline{S}}_k\,\underline{F}_k\,\dot{\underline{X}} \qquad \text{(C .2.10)}$$

where $\underline{S}_k$ denotes the random matrix

$$\tilde{\underline{S}}_k = \begin{bmatrix} S_1 & & & 0 \\ & S_2 & & \\ & & \ddots & \\ 0 & & & S_k \end{bmatrix} \qquad \text{(C .2.11)}$$

It follows at once from (C.2.11) that

$$E[\hat{\underline{X}}_{\tau k} - \underline{X}_{\tau k}] = -\Delta T\,[\underline{F}_k'\,\underline{Q}_k\,\underline{F}_k]^{-1}\,\underline{F}_k'\,\underline{Q}_k\,[E\,\{\tilde{\underline{S}}_k\}]\,\underline{F}_k\,\dot{\underline{X}}$$

$$= -\Delta T\,\frac{(k-1)}{2}\,[\underline{F}_k'\,\underline{Q}_k\,\underline{F}_k]^{-1}\,\underline{F}_k'\,\underline{Q}_k\,\underline{F}_k\,\dot{\underline{X}}$$

$$= -\Delta T\,\frac{(k-1)}{2}\,\dot{\underline{X}}\ . \qquad \text{(C .2.12)}$$

Step 3: The Covariance Matrix of (4.3.13) About its Mean

For an aircraft moving the α-direction with constant velocity V_α

$$\dot{\underline{X}} = V_\alpha \begin{bmatrix} 1 \\ 0 \\ 0 \end{bmatrix} \qquad \text{(C .2.13)}$$

$$\hat{\underline{X}}_{\tau k} - \underline{X}_{\tau k} = -(V_\alpha \Delta T)[\underline{F}_k'\,\underline{Q}_k\,\underline{F}_k]^{-1}\,\underline{F}_k'\,\underline{Q}_k\,\tilde{\underline{S}}_k\,\underline{F}_k \begin{bmatrix} 1 \\ 0 \\ 0 \end{bmatrix} \qquad \text{(C .2.14)}$$

The deviation $\underline{\delta}_x$ of the motional error from its mean is

$$\underline{\delta}_x = -(V_\alpha \Delta T)[\underline{F}_k'\,\underline{Q}_k\,\underline{F}_k]^{-1}\,\underline{F}_k'\,\underline{Q}_k(\tilde{\underline{S}}_k - \bar{\underline{S}}_k)\,\underline{F}_k \begin{bmatrix} 1 \\ 0 \\ 0 \end{bmatrix} \qquad \text{(C.2.15)}$$

where $\bar{\underline{S}}_k$ denotes the expectation of $\tilde{\underline{S}}_k$. The covariance matrix for $\underline{\delta}_x$ takes the form

$$E[\underline{\delta}_x\,\underline{\delta}_x'] = \underline{J}\,\underline{\Omega}\,\underline{J}' \qquad \text{(C.2.16)}$$

where

$$\underline{J} = -(V_\alpha \Delta T)\,[\underline{F}_k'\,\underline{Q}_k\,\underline{F}_k]^{-1}\,\underline{F}_k'\,\underline{Q}_k \qquad \text{(C .2.17)}$$

$$\underline{\Omega} = E\left\{(\tilde{\underline{S}}_k - \overline{\underline{S}}_k)\,\underline{F}_k \begin{bmatrix}1\\0\\0\end{bmatrix}[1\ \ 0\ \ 0]\,\underline{F}_k'\,(\tilde{\underline{S}}_k - \overline{\underline{S}}_k)\right\} \qquad \text{(C .2.18)}$$

The typical element of $\underline{\Omega}$ is given by

$$\Omega_{ij} = f_{i1}\,f_{j1}\,E[(S_i - \overline{S}_i)(S_j - \overline{S}_j)] \qquad \text{(C .2.19)}$$

where f_{i1} denotes the ith element in the first column of $\underline{F}_k$. Use of (C.2.8) and (C.2.9) in (C.2.19) shows that

$$\Omega_{ij} = \begin{cases} (f_{i1})^2\left[\dfrac{k(k+1)}{12} - \dfrac{k+1}{12}\right] & (i=j) \\ f_{i1}\,f_{j1}\left[0 - \dfrac{k+1}{12}\right] & (i\neq j) \end{cases} \qquad \text{(C .2.20)}$$

Consequently

$$\Omega = + \frac{k(k+1)}{12} \underline{\pi}$$

$$- \frac{(k+1)}{12} \underline{F}_k \begin{bmatrix} 1 \\ 0 \\ 0 \end{bmatrix} [1 \quad 0 \quad 0] \underline{F}_k' \qquad \text{(C.2.21)}$$

where

$$\underline{\pi} = \begin{bmatrix} (f_{11})^2 & & & 0 \\ & (f_{21})^2 & & \\ & & \ddots & \\ 0 & & & (f_{k1})^2 \end{bmatrix} \qquad \text{(C.2.22)}$$

Use of (C.2.21) and (C.2.17) in (C.2.16) gives

$$E[\underline{\delta}_x \underline{\delta}_x'] = + \frac{k(k+1)}{12} (V_\alpha \Delta T)^2 [\underline{F}_k' \underline{Q}_k \underline{F}_k]^{-1} \underline{F}_k' \underline{Q}_k \underline{\pi} \underline{Q}_k \underline{F}_k [\underline{F}_k' \underline{Q}_k \underline{F}_k]^{-1}$$

$$- \frac{k+1}{12} (V_\alpha \Delta T)^2 \begin{bmatrix} 1 & 0 & 0 \\ 0 & 0 & 0 \\ 0 & 0 & 0 \end{bmatrix} \qquad \text{(C.2.23)}$$

Step 4: Evaluation of Eq. (C.2.23)

As an illustration, the expression (C.2.23) is evaluated for the satellite deployment shown in Fig. 4.3, assuming

$$\sigma_1^2 = \sigma_2^2 = \cdots \sigma_k^2 = \sigma^2 \qquad \text{(C.2.24)}$$

Note that

$$k = 9 \tag{C .2.25}$$

for the constellation of Fig. 4.3.

The matrix $\underline{F}_k$ of unit vectors is as follows

$$\underline{F}_k = \begin{bmatrix} 0.866 & 0 & 0.500 \\ -0.866 & 0 & 0.500 \\ 0.500 & 0 & 0.866 \\ -0.500 & 0 & 0.866 \\ 0 & -0.866 & 0.500 \\ 0 & 0.866 & 0.500 \\ 0 & -0.500 & 0.866 \\ 0 & 0.500 & 0.866 \\ 0 & 0 & 1.000 \end{bmatrix} \tag{C .2.26}$$

The $\underline{Q}_k$ matrix takes the form

$$\underline{Q}_k = \frac{1}{\sigma^2} \left[I - \frac{1}{k} \underline{1} \underline{1}' \right] \tag{C .2.27}$$

Premultiplication of (C.2.26) by (C.2.27) yields

$$\underline{Q}_k \underline{F}_k = \frac{1}{\sigma^2} \begin{bmatrix} 0.866 & 0 & -0.218 \\ -0.866 & 0 & -0.218 \\ 0.500 & 0 & 0.148 \\ -0.500 & 0 & 0.148 \\ 0 & -0.866 & -0.218 \\ 0 & 0.866 & -0.218 \\ 0 & -0.500 & 0.148 \\ 0 & 0.500 & 0.148 \\ 0 & 0 & 0.282 \end{bmatrix} \qquad \text{(C .2.28)}$$

It follows from (C.2.26) that

$$\underline{\pi} = \begin{bmatrix} 0.75 & & & & & & & & \\ & 0.75 & & & & & & & \\ & & 0.25 & & & & & & \\ & & & 0.25 & & & & & \\ & & & & 0 & & & & \\ & & & & & 0 & & & \\ & & & & & & 0 & & \\ & & & & & & & 0 & \\ & & & & & & & & 0 \end{bmatrix} \qquad \text{(C .2.29)}$$

The products $\underline{F}_k' \underline{Q}_k \underline{F}_k$ and $\underline{F}_k' \underline{Q}_k \underline{\pi} \underline{Q}_k \underline{F}_k$ can straightforwardly be calculated from (C.2.26) - (C.2.29). The results are

$$\underline{F}_k' \underline{Q}_k \underline{F}_k = \frac{1}{\sigma^2} \begin{bmatrix} 2 & 0 & 0 \\ 0 & 2 & 0 \\ 0 & 0 & 0.357 \end{bmatrix} \qquad \text{(C .2.30)}$$

$$\underline{F}_k' \underline{Q}_k \underline{\pi} \underline{Q}_k \underline{F}_k = \frac{1}{\sigma^4} \begin{bmatrix} 1.25 & 0 & 0 \\ 0 & 0 & 0 \\ 0 & 0 & 0.0824 \end{bmatrix} \qquad \text{(C .2.31)}$$

Consequently,

$$[\underline{F}_k' \underline{Q}_k \underline{F}_k]^{-1} \underline{F}_k' \underline{Q}_k \underline{\pi} \underline{Q}_k \underline{F}_k [\underline{F}_k' \underline{Q}_k \underline{F}_k]^{-1} =$$

$$\begin{bmatrix} 0.313 & 0 & 0 \\ 0 & 0 & 0 \\ 0 & 0 & 0.646 \end{bmatrix} \qquad \text{(C .2.32)}$$

Substitution of (C.2.32) and (C.2.25) in (C.2.23) gives

$$E[\underline{\delta}_k \underline{\delta}_k'] = (V_\alpha \Delta\tau)^2 \begin{bmatrix} 1.515 & 0 & 0 \\ 0 & 0 & 0 \\ 0 & 0 & 4.845 \end{bmatrix} \qquad \text{(C .2.33)}$$

Therefore the rms deviation of the estimate (4.3.7) from its mean are given by

$$\sigma_\alpha = 1.231\ (V_\alpha \Delta\tau) \tag{C.2.34}$$

$$\sigma_\beta = 0 \tag{C.2.35}$$

$$\sigma_\gamma = 2.201\ (V_\alpha \Delta\tau) \tag{C.2.36}$$

If V_α = 150 mph (220 fps) and ΔT = 0.05 sec (as in Section 3.1), then

$$\sigma_\alpha = 13.5 \text{ ft} \tag{C.2.37}$$

$$\sigma_\beta = 0 \tag{C.2.38}$$

$$\sigma_\gamma = 24.5 \text{ ft} \tag{C.2.39}$$

If V_α = 650 mph and ΔT = 0.05 sec, then

$$\sigma_\alpha = 58.5 \text{ ft} \tag{C.2.40}$$

$$\sigma_\beta = 0 \tag{C.2.41}$$

$$\sigma_\gamma = 104.9 \text{ ft} \tag{C.2.42}$$

C.3 SEQUENTIAL LEAST SQUARES SOLUTION OF EQ. (4.4.2)

The least squares solution of Eq. (4.4.2) is developed in the following steps:

1. The variable T_0 is eliminated from the Eqs. (4.4.1).
2. The elimination procedure has a side effect of replacing the uncorrelated errors $\varepsilon_1, \varepsilon_2, \cdots, \varepsilon_k$ by correlated errors. Thus a linear transformation is applied to the new equations to de-correlate the errors.
3. A sequential procedure is formulated for calculating the least squares solution $\underline{\chi}$ of the resulting equations.
4. The procedure is recast in a form suitable for practical calculations.

While Steps 1-3 differ from the usual procedure for determining the least squares solution of Eq. (4.4.2), it can be shown that they produce exactly the same result.

Instead of carrying the factor $e^{-(\tau_k-\tau_i)/\tau}$ in Eq. (4.4.5) through the development, it is simpler to assume that the errors ε_i have variances of $e^{(\tau_k-\tau_i)/\tau}\ (\sigma_i)^2$. Accordingly, the following matrix is used in place of (4.2.1)

$$\underline{P_k} = \begin{bmatrix} e^{(\tau_k-\tau_1)/\tau}\sigma_1^2 & & \bigcirc \\ & e^{(\tau_k-\tau_2)/\tau}\sigma_2^2 & \\ & & \ddots \\ \bigcirc & & e^{(\tau_k-\tau_k)/\tau}\sigma_k^2 \end{bmatrix} \qquad (C.3.1)$$

or equivalently

$$\underline{P}_k = e^{+\tau_k/\tau}\,\underline{G}_k \qquad \text{(C.3.2)}$$

where

$$\underline{G}_k = \begin{bmatrix} e^{-\tau_1/\tau}\sigma_1^2 & & & \\ & e^{-\tau_2/\tau}\sigma_2^2 & & \\ & & \ddots & \\ & & & e^{-\tau_k/\tau}\sigma_k^2 \end{bmatrix} \qquad \text{(C.3.3)}$$

Step 1: Elimination of T_0

The variable T_0 can be eliminated from Eq. (4.4.2) by premultiplying (4.4.2) by the matrix

$$\underline{H}_k = \underbrace{\begin{bmatrix} 1 & -1 & & 0 \\ & 1 & -1 & \\ & & \ddots & \\ 0 & & & 1 \quad -1 \end{bmatrix}}_{k \text{ columns}} \Bigg\} \; k\text{-}1 \text{ rows} \qquad \text{(C.3.4)}$$

The result is

$$\underline{H}_k\,\underline{K}_k = \underline{H}_k\,\underline{N}_k\,\underline{\chi} + c\,\underline{H}_k\,\underline{\varepsilon}_k \quad . \qquad \text{(C.3.5)}$$

Step 2: Decorrelation

The covariance matrix for the error term $c\underline{H}_k \underline{\varepsilon}_k$ in Eq. (C.3.5) is given by

$$\begin{aligned} \underline{J}_k &= c^2 \, E[\underline{H}_k \underline{\varepsilon}_k \underline{\varepsilon}_k' \underline{H}_k'] \\ &= c^2 \, \underline{H}_k \underline{P}_k \underline{H}_k' \\ &= c^2 \, e^{\tau_k/\tau} \, \underline{H}_k \underline{G}_k \underline{H}_k' \end{aligned} \tag{C.3.6}$$

The matrix $\underline{J}_k$ can be diagonalized by the congruence transformation

$$\underline{L}_k \underline{J}_k \underline{L}_k' = \underline{D}_k \quad (= \text{diagonal}) \tag{C.3.7}$$

with

$$\underline{L}_k = \begin{bmatrix} 1 & & & \\ \left(\frac{\Sigma_1}{\Sigma_2}\right) & 1 & & \\ \left(\frac{\Sigma_1}{\Sigma_3}\right) & \left(\frac{\Sigma_2}{\Sigma_3}\right) & 1 & \\ \vdots & \vdots & \vdots & \ddots \\ \left(\frac{\Sigma_1}{\Sigma_{k-1}}\right) & \left(\frac{\Sigma_2}{\Sigma_{k-1}}\right) & \left(\frac{\Sigma_3}{\Sigma_{k-1}}\right) \cdots & 1 \end{bmatrix} \quad \begin{matrix} \\ \\ \\ \\ \} \text{ k-1 rows} \end{matrix} \tag{C.3.8}$$

k-1 columns

where the notation $\sum_j$ means

$$\sum_j = \sum_{i=1}^{j} 1/g_{ii} = \sum_{i=1}^{j} e^{\tau_i/\tau}/(\sigma_i)^2 \qquad \text{(C.3.9)}$$

and g_{ii} denotes the i-i element of the matrix (C.3.3).
Specifically,

$$\underline{D}_k = c^2 \, e^{\tau_k/\tau} \, \underline{L}_k \, \underline{H}_k \, \underline{G}_k \, \underline{H}'_k \, \underline{L}'_k$$

$$= c^2 \, e^{\tau_k/\tau} \begin{bmatrix} \left(\frac{1}{\Sigma_1} + g_{22}\right) & & \bigcirc \\ & \left(\frac{1}{\Sigma_2} + g_{33}\right) & \\ & & \ddots \\ \bigcirc & & \left(\frac{1}{\Sigma_{k-1}} + g_{k,k}\right) \end{bmatrix} \begin{matrix} \} \text{k-1 rows} \\ \\ \\ \\ \underbrace{\qquad\qquad}_{\text{k-1 columns}} \end{matrix} \qquad \text{(C.3.10)}$$

Thus the error term in Eq. (C.3.5) can be de-correlated by pre-multiplying Eq. (C.3.5) by $\underline{L}_k$. The resulting equation takes the form

$$\underline{Y}_k = \underline{A}_k \, \underline{X} + \underline{\delta}_k \qquad \text{(C.3.11)}$$

where

$$\underline{Y}_k = \underline{L}_k \underline{H}_k \underline{K}_k \qquad (k-1) \times 1 \qquad \text{(C.3.12)}$$

$$\underline{A}_k = \underline{L}_k \underline{H}_k \underline{N}_k \qquad (k-1) \times 6 \qquad \text{(C.3.13)}$$

$$\underline{\delta}_k = c\, \underline{L}_k \underline{H}_k \underline{\varepsilon}_k \qquad (k-1) \times 1 \qquad \text{(C.3.14)}$$

The covariance matrix $E[\underline{\delta}_k \underline{\delta}_k']$ is given by (C.3.10).

Step 3: Sequential Form of Least Squares Solution

The least squares solution $\underline{\chi}$ of (C.3.11) minimizes the error measure

$$E_k'(\underline{\chi}) = \underline{\delta}_k' \underline{D}_k^{-1} \underline{\delta}_k$$

$$= [\underline{Y}_k - \underline{A}_k \underline{\chi}]' \underline{D}_k^{-1} [\underline{Y}_k - \underline{A}_k \underline{\chi}] \qquad \text{(C.3.15)}$$

To develop a sequential procedure for calculating the minimizing vector $\underline{\chi}$ it is necessary to express $E_k'(\underline{\chi})$ in terms of the error measure E_{k-1}' for the preceding measurement.

The matrices $\underline{L}_k$, $\underline{H}_k$, $\underline{N}_k$ and $\underline{K}_k$ can be expressed in terms of the corresponding matrices $\underline{L}_{k-1}$, $\underline{H}_{k-1}$, $\underline{N}_{k-1}$, and $\underline{K}_{k-1}$ for the preceding measurement as follows:

$$\underline{L}_k = \left[\begin{array}{c|c} \underline{L}_{k-1} & 0 \\ \hline \underline{\ell}_k & \end{array}\right] , \qquad \underline{H}_k = \left[\begin{array}{c|c} \underline{H}_{k-1} & 0 \\ \hline \underline{h}_k & \end{array}\right] \tag{C.3.16-17}$$

$$\underline{N}_k = \left[\begin{array}{c|c} \underline{N}_{k-1} & \underline{M}_k \\ \hline \underline{n}_k & \end{array}\right] , \qquad \underline{K}_k = \left[\begin{array}{c} \underline{K}_{k-1} \\ \hline \underline{k}_k \end{array}\right] \tag{C.3.18-19}$$

where

$$\underline{M}_k = \begin{bmatrix} 1 & 0 & 0 & -(\tau_k-\tau_{k-1}) & 0 & 0 \\ 0 & 1 & 0 & 0 & -(\tau_k-\tau_{k-1}) & 0 \\ 0 & 0 & 1 & 0 & 0 & -(\tau_k-\tau_{k-1}) \\ 0 & 0 & 0 & 1 & 0 & 0 \\ 0 & 0 & 0 & 0 & 1 & 0 \\ 0 & 0 & 0 & 0 & 0 & 1 \end{bmatrix} \tag{C.3.20}$$

$$\underline{\ell}_k = \left\{ \left(\frac{\Sigma_1}{\Sigma_{k-1}}\right) , \left(\frac{\Sigma_2}{\Sigma_{k-1}}\right) , \cdots , \left(\frac{\Sigma_{k-2}}{\Sigma_{k-1}}\right) , 1 \right\} \tag{C.3.21}$$

$$\underline{h}_k = \underbrace{[0 \quad \cdot \quad \cdot \quad \cdot \quad 0 \quad +1 \quad -1]}_{k} \tag{C.3.22}$$

$$\underline{n}_k = \underbrace{[\underline{i}_k \,|\, 0 \quad 0 \quad 0]}_{6} \tag{C.3.23}$$

$$\underline{k}_k = c\tau_k - c \sum_{i=1}^{k} \Delta\tau_{i-1,i} - r_k \tag{C.3.24}$$

Use of Eqs. (C.3.16) - (C.3.19) in Eqs. (C.3.12) and (C.3.13) shows that $\underline{Y}_k$ and $\underline{A}_k$ can be expressed in terms of $\underline{Y}_{k-1}$ and $\underline{A}_{k-1}$ as follows:

$$\underline{Y}_k = \left[\frac{\underline{Y}_{k-1}}{y_k}\right] \tag{C.3.25}$$

$$\underline{A}_k = \left[\frac{\underline{A}_{k-1}\ \underline{M}_k}{\underline{a}_k}\right] \tag{C.3.26}$$

where

$$y_k = \underline{\ell}_k\ \underline{H}_k\ \underline{K}_k \tag{C.3.27}$$

$$\underline{a}_k = \underline{\ell}_k\ \underline{H}_k\ \underline{N}_k \qquad (1\text{x}6) \tag{C.3.28}$$

Examination of Eq. (C.3.10) shows that $\underline{D}_k$ can be expressed in terms of $\underline{D}_{k-1}$ as follows:

$$\underline{D}_k = \left[\begin{array}{c|c} e^{(\tau_k-\tau_{k-1})/\tau}\ \underline{D}_{k-1} & 0 \\ \hline 0 & d_k \end{array}\right] \tag{C.3.29}$$

where

$$d_k = c^2 \, e^{\tau_k/\tau}\left[\frac{1}{\Sigma_{k-1}} + g_{k,k}\right] \qquad \text{(C.3.30)}$$

Substitution of Eqs. (C.3.25), (C.3.26), and (C.3.29) in Eq. (C.3.15) gives

$$E'_k(\underline{X}) = e^{-(\tau_k-\tau_{k-1})/\tau}\,[\underline{Y}_{k-1} - \underline{A}_{k-1}\,\underline{M}_k\,\underline{X}]'\,\underline{D}_{k-1}^{-1}\,[\underline{Y}_{k-1} - \underline{A}_{k-1}\,\underline{M}_k\underline{X}] + \frac{1}{d_k}(y_k - \underline{a}_k\,\underline{X})^2 \qquad \text{(C.3.31)}$$

Equation (C.3.15) now can be re-written in terms of the error measure E_{k-1} for the preceding measurement, as follows:

$$E'_k(\underline{X}) = e^{-(\tau_k-\tau_{k-1})/\tau}\,E'_{k-1}(\underline{M}_k\,\underline{X}) + \frac{1}{d_k}(y_k - \underline{a}_k\,\underline{X})^2 \qquad \text{(C.3.32)}$$

The quadratic form $E_{k-1}(\underline{M}_k\,\underline{X})$ can be expressed in a Taylor series about $\hat{\underline{X}}_{k-1}$ as follows

$$E'_{k-1}(\underline{M}_k\,\underline{X}) = E'_{k-1}(\hat{\underline{X}}_{k-1}) + (\underline{M}_k\underline{X} - \hat{\underline{X}}_{k-1})'\underline{\Lambda}_{k-1}^{-1}(\underline{M}_k\underline{X} - \hat{\underline{X}}_{k-1}) \qquad \text{(C.3.33)}$$

Note that the first order term is absent since $E'_{k-1}(\ \ )$ assumes a minimum value at $\hat{\underline{X}}_{k-1}$. Use of (C.3.33) in (C.3.32) yields

$$E_k'(\underline{x}) = e^{-(\tau_k-\tau_{k-1})/\tau}[\underline{E}_{k-1}'(\hat{\underline{x}}_{k-1}) + (\underline{M}_k \underline{x} - \hat{\underline{x}}_{k-1})' \underline{\Lambda}_{k-1}^{-1}(M_k \underline{x} - \hat{x}_{k-1})]$$

$$+ \frac{1}{d_k}(y_k - \underline{a}_k \underline{x})^2 \qquad \text{(C.3.34)}$$

Straightforward minimization of (C.3.34) yields the basic equation for calculating $\underline{x}_k$ from $\underline{x}_{k-1}$; namely

$$\hat{\underline{x}}_k = \underline{M}_k^{-1} \hat{\underline{x}}_{k-1} + \frac{1}{d_k} \Lambda_k \underline{a}_k'(y_k - \underline{a}_k \underline{M}_k^{-1} \hat{\underline{x}}_{k-1}) \qquad \text{(C.3.35)}$$

where

$$\underline{\Lambda}_k = \left[e^{-(\tau_k-\tau_{k-1})/\tau} \underline{M}_k' \underline{\Lambda}_{k-1}^{-1} \underline{M}_k + \frac{1}{d_k} \underline{a}_k' \underline{a}_k\right]^{-1} \qquad \text{(C.3.36)}$$

Step 4: Practical Calculations

To minimize round-off errors, it is desirable to change variables in (C.3.35) as follows

$$\hat{\underline{x}}_k = \underline{R}^{-1} \underline{S}_k \qquad \text{(C.3.37)}$$

where

$$\underline{R} = \left[\begin{array}{c|c} \begin{matrix} 1 & & \\ & 1 & \\ & & 1 \end{matrix} & \begin{matrix} 0 \\ \\ T \end{matrix} \\ \hline \begin{matrix} 0 & & \end{matrix} & T \end{array}\right] \qquad \text{(C.3.38)}$$

and T denotes a normalizing time. In addition, it is advantageous to introduce

a normalizing variance $(\sigma^*)^2$. Use of (C.3.37) in (C.3.35), pre-multiplication of the result by $\underline{R}$, and some manipulation of (C.3.36) leads to the following counterparts of (C.3.35) and (C.3.36)

$$\underline{S}_k = \underline{\tilde{M}}_k^{-1} \underline{S}_{k-1} + \left(\frac{\sigma^*}{\sigma_k}\right)^2 \phi_k \underline{\Gamma}_k \underline{b}_k' (y_k - \underline{b}_k \underline{\tilde{M}}_k^{-1} \underline{S}_{k-1}) \tag{C.3.39}$$

$$\underline{\Gamma}_k^{-1} = e^{-(\tau_k - \tau_{k-1})/\tau} \underline{\tilde{M}}_k' \underline{\Gamma}_{k-1}^{-1} \underline{\tilde{M}}_k + \left(\frac{\sigma^*}{\sigma_k}\right)^2 \phi_k \underline{b}_k' \underline{b}_k \tag{C.3.40}$$

where

$$\underline{\tilde{M}}_k^{-1} = \underline{R} \underline{M}_k^{-1} \underline{R}^{-1} \tag{C.3.41}$$

$$\phi_k = \Sigma_{k-1}/\Sigma_k \tag{C.3.42}$$

$$\underline{\Gamma}_k = \frac{1}{(c\sigma^*)^2} \underline{R} \underline{\Lambda}_k \underline{R} \tag{C.3.43}$$

$$\underline{b}_k' = \underline{R}^{-1} \underline{a}_k' \tag{C.3.44}$$

The quantities ϕ_k, y_k, and $\underline{b}_k$ can be calculated in a sequential manner by using relationships

$$\phi_k = \frac{e^{-(\tau_k - \tau_{k-1})/\tau} (\sigma_k/\sigma_{k-1})^2}{\left[1 + e^{-(\tau_k - \tau_{k-1})/\tau} (\sigma_k/\sigma_{k-1})^2 - \phi_{k-1}\right]} \tag{C.3.45}$$

$$y_k = \phi_{k-1}\, y_{k-1} + [c(\tau_{k-1} - \tau_k + \Delta\tau_{k-1,k}) - r_{k-1} + r_k] \qquad (C.3.46)$$

$$\underline{b}_k = \phi_{k-1}\, \underline{b}_{k-1} + [(\underline{i}_{k-1} - \underline{i}_k) \vdots \frac{1}{T}(\tau_{k-1} - \tau_k)\, \underline{i}_{k-1}] \qquad (C.3.47)$$

[to verify Eqs. (C.3.45) - (C.3.47) simply substitute the definitions of ϕ_k, y_k, and $\underline{b}_k$] .

Once ϕ_k, y_k, and $\underline{b}_k$ are available, $\underline{\Gamma}_k$ and $\underline{S}_k$ can be calculated from Eqs. (C.3.39) and (C.3.40); then $\underline{\chi}$ can be calculated from Eq. (C.3.37).

The flowchart in Fig. 4.6 summarizes all necessary calculations.

APPENDIX D

SATELLITE DATA LINK

The baseline SAT system uses the DAB transponder to send position estimates to the ground. It is also possible to report multilateration position estimates from the aircraft to the ground via satellite relay.

In this appendix, we discuss the error probability of a system wherein the aircraft reports its position at random intervals. A synchronous satellite relays the aircraft reports to a central ground ATC communication center. The avionics required for communications between aircraft and satellite are discussed in references [10,11]. The chief limitation of random reporting is multiple access noise, the garbling resulting from simultaneous reception of communications from several aircraft. By using multiple frequency channels, and a satellite antenna with multiple beams, it is possible to keep the probability of message error $P_e \leq 0.1$.

Let us consider a candidate link design for reporting position at random times with an average reporting period of 10 seconds. The candidate message contains 90 DPSK chips of 1 μsec duration, for a total message length of 90 μsec. The chip rise time is to be less than 100 nsec. The first 16 chips are a coded sequence common to all aircraft which are used to establish timing synchronization. The remaining 74 chips are used to transmit 20 bits of identity and 37 bits of position information. Sixteen chips have been reserved for coding purposes.

Table D.1 presents an aircraft-to-satellite link power budget. To achieve an rms synchronization error of less than 15 nsec it is necessary to have a

sequence signal-to-noise ratio at the satellite receiver of 21 dB [18]. To achieve a probability of error per chip due to receiver noise of less than 2×10^{-4}, it is necessary to have a received signal-to-noise ratio per chip (E_c/N_o) of at least 9 dB. These two requirements are compatible since 16 chips are used for synchronization. However, to account for suboptimum DPSK demodulation, we should have E_c/N_o of 11 dB. Many of the terms in the power budget are the same as in Table 3.1. We have budgeted a noise power density of -201 dBW/Hz, corresponding to a 600°K equivalent noise temperature. To guarantee the required signal-to-noise ratio, the aircraft must transmit 600 W. Such a requirement is within the reach of current technology.

We wish to bound the message error probability $P_e < 0.1$, and find the capacity of this communications link. The message error probability due to noise, P_{emn}, can be bounded by

$$P_{emn} \leq 90\ P_{e,c} \leq 0.018$$

where we have already noted in the power budget discussion that we can bound the chip error probability by $P_{e,c} \leq 2\times10^{-4}$. Therefore, we can assure $P_e < 0.1$ by bounding the garble probability

$$P_g \leq 0.082 \qquad \text{(D.1)}$$

where a garble is taken to be any message overlap.

TABLE D.1

AIRCRAFT-TO-SATELLITE POWER BUDGET

Transmitter Peak Power 600 W (minimum at antenna)	28 dBW
Minimum Aircraft Antenna Gain	-1 dB
Maximum Path Loss	-192 dB
Atmospheric Fading	-1 dB
Peak Satellite Antenna Gain	42 dB
Off Boresight Loss	-3 dB
Thermal Distortion	-2 dB
Antenna Feed Shadowing	-1 dB
Received Peak Power	-130 dBW
Noise Power Density (600°K equiv.)	-201 dBW/Hz
Received Peak Power-to- Noise Power Ratio	71 dBHz
Chip Duration (1 μsec)	-60 dB sec
E/N_0 minimum	11 dB

We wish to use the same aircraft antenna for receiving timing pulses and transmitting position estimates. In Section III, we explained that each satellite and each beam transmit in sequence. Each aircraft receiver has to receive satellite transmissions only seven percent of the time. After the receiver acquires the satellite epoch time, more than ninety percent of the time will be available for reporting position estimates. Specifically, during each 10 sec interval, more than 9 sec will be available for the aircraft to transmit to the satellite. In this candidate scheme, the aircraft computer chooses a transmission time at random from the 9 available seconds.

The capacity N_c for the link can be bounded in the following way: If two messages of length τ are uniformly distributed over an interval T, the probability p_2 that this pair of messages partially overlap is

$$p_2 = \frac{2\tau}{T} \tag{D.2}$$

Now consider N messages of length τ, each independently uniformly distributed over the interval T. Pick any one of the N messages. Using the union bound, the probability p_n that one of the (N-1) remaining messages partially overlap the chosen message is bounded by

$$p_n \leq (N-1)\, p_2 < \frac{2N}{T} \tag{D.3}$$

We can find the capacity by setting $N = N_c$, $p_n = 0.0816$ (see (D.1)), $\tau = 90 \times 10^{-6}$ sec, and $T = 9.1$ sec. Then

$$N_c = \frac{p_n T}{2\tau} = 4100 \tag{D.4}$$

The link capacity can be increased in the following way: The chip bandwidth is approximately 1 MHz. Suppose 10 different adjacent frequencies, spaced 1 MHz apart, were assigned to an equal number of aircraft. If the allowable deviations from assigned frequency was limited to $\pm$ 3 MHz, the total frequency allocation would be 16 MHz. The ground receiver would have to monitor a bank of matched filters over this range of frequencies, choosing the frequency as well as the time at which the synchronization sequence peaked. We model the filters as perfect 1 MHz bandpass filters. Only a small fraction of the total equipped aircraft would be using the position reporting system at any one time. We wish to estimate the capacity N_T of the entire system, taking into account the random distribution of aircraft transmitter frequencies.

We model the capacity problem in the following way: The capacity of a 1 MHz bandpass channel is 4100 aircraft. We model the aircraft transmitter frequencies as being uniformly distributed over a 10 MHz passband (i.e., we ignore end effects). Then the probability of an aircraft transmitter frequency being within any 1 MHz passband interior to the 10 MHz passband is $p = 0.1$. Let N_T be the number of aircraft in an interior 1 MHz passband. The mean of N_1 is

$$\bar{N}_1 = N_T p \tag{D.5}$$

and the variance of N_1 is

$$E[(N_1 - \bar{N}_1)^2] = N_T p(1 - p) \tag{D.6}$$

We will require the probability

$$Pr\{N_1 > 4100\} < 10^{-6} \tag{D.7}$$

Using the central limit theorem, (D.7) is satisfied if [17]

$$N_T p + 5[N_T p(1 - p)]^{1/2} = 4100 \tag{D.8}$$

Using (D.8), (D.7) will be satisfied by

$$N_T = 38{,}000 \tag{D.9}$$

The peak instantaneous airborne count may exceed 38,000 aircraft during the 1990's, but a majority of the aircraft would be under DABS surveillance. DABS all-call lockout could be utilized to prevent aircraft from reporting position via satellite relay when they are under DABS control. Using DABS lockout, this system would have enough coverage to maintain cooperative surveillance on all CONUS aircraft not covered by DABS. In estimating the capacity, we have ignored the beneficial effects on multiple access noise of the narrow satellite antenna beamwidth. At the edge of the beam footprint, received power may be the same on two beams. However, with 10 beams covering CONUS, East Coast aircraft would not garble West Coast aircraft even if the transmissions were received simultaneously.* Therefore, the bound on message error probability at "capacity" is a conservative bound.

*A signal-to-interference ratio of 14 dB is equivalent to a 1 dB increase in noise power in the absence of interference [19]. The beamwidth at -14 dB is approximately 1.9 times the beamwidth at -3 dB.